MASTER'S THESIS | LUND UNIVERSITY 2016

Robust Route Prediction in Raster Maps

Sebastian Fabian

Department of Computer Science
Faculty of Engineering LTH

ISSN 1650-2884
LU-CS-EX 2016-07

Robust Route Prediction in Raster Maps

(Real Time Linear Topography for Look-Ahead Control)

Sebastian Fabian
sjlfabian@gmail.com

March 29, 2016

Master's thesis work carried out at Scania CV AB.

Supervisors: Per Sahlholm, per.sahlholm@scania.com
Flavius Gruian, flavius.gruian@cs.lth.se

Examiner: Jonas Skeppstedt, jonas.skeppstedt@cs.lth.se

Abstract

By adapting gear changes and cruise control of a Heavy Duty Vehicle (HDV) to road inclination, fuel and time savings can be achieved. In this thesis is presented a novel method of predicting the upcoming road topography, by constructing a geographical and topographical self-learning map from which a route prediction is made. The system is designed to simultaneously produce the desired road grade output in real time and update the map each time an area is driven through, making the map more accurate as more data is collected. Special considerations are given to the memory and processing constraints of embedded automotive control hardware.

Keywords: raster map, route prediction, data structure, embedded, automotive, heat map, GIS, topography

Acknowledgments

Thanks to Scania for giving me this opportunity.

To my enthusiastic coworkers at REV at Scania R&D, for making my time there memorable. I would like to especially thank Per Sahlholm for his guidance and inspiration.

Contents

Glossary

ADAS
: Advanced Driver Assistance System. Digital system to assist the driver by enhancing, augmenting or simplifying driving functions.

HDV
: Heavy Duty Vehicle

ECU
: Electronic Control Unit. A generic designation for a digital computer unit in an automotive context, typically used for ignition control, gearbox control and other digital functions of the vehicle.

Raster
: A dot matrix data structure that stores information about some entity as a matrix of discrete values, each representing a fixed size portion.

Pixel
: The value that makes up the each element in a raster dot matrix.

Horizon
: A predicted route of some length.

Tile
: A square cluster of pixels, making up a subset of a raster dot matrix. A smaller portion than the entire raster dot matrix, although large than a single pixel.

Node map
: A map system made up of interconnected nodes. Typically used in most commerical map applications, including navigation.

GPS
: Global Positioning System. A standard to determine one's location upon the earth based on triangulation with satellites.

(Adaptive) cruise control
Automatic control system intended to control vehicle speed. Adaptive cruise control systems may change the speed setting to respond to surrounding conditions whereas plain cruise control keeps a set value.

CAN
Controller Area Network. Network connection standard for interconnected distributed systems, typically used in vehicles to communicate between ECUs.

KDE
Kernel Density Estimation. A method of constructing graph-based maps.

GIS
Geographic Information Science. The discipline of geographic information system study.

WGS84
World Geodetic System 84. Standardized coordinate system for mapping the earth.

GPS trace
A series of GPS coordinates, forming a single path of travel data.

Heat map
A map structure that consists of a single value for each point, typically visiting frequency.

KiB, MiB, GiB
Prefixed units for unambiguously describing amounts of data in prefix steps of 1024 bytes, as described in IEC [1].

Chapter 1

Introduction

In today's society of rising demand of transport services and their efficacy, fuel efficiency and mechanical reliability are more important than ever before and are a vital part of the everyday business for any logistics operation. In order to meet the needs of this increasingly global and connected society, smart ways to minimize fuel consumption and increase dependability of commercial fleets are highly desirable. This is evident by the rise of sophisticated Advanced Driver Assistance Systems (ADAS), such as autonomous emergency brakes and adaptive cruise control that meet a range of goals, such as minimizing human error and maximizing operational efficiency. Other approaches, that lack interaction from the driver, come in all shapes and forms, both digital and mechanical. Together, these technologies represent a hallmark of the modern automotive industry.

One such non-interactive technology for saving fuel is road prediction and using derived data in the distributed network of Electronic Control Units (ECU) to improve several integrated functions of the vehicle. One such application is cruise control that adapts to the road ahead. By, for instance, letting go of the throttle before a crest, velocity increase due to the upcoming slope can be minimized which can prevent unnecessary braking and thus save fuel. Similarly, a throttle increase before an ascent can improve efficiency by minimizing the temporary slowdown. Another desirable application for such technology is gear shift timing. By shifting down just before the ascent, a heavily loaded commercial vehicle can prepare for increased torque output beforehand which can, in some cases, eliminate the need for a mid-ascent gear shift. Additionally, by saving the time it takes to perform the actual shift, doing so in anticipation allows preservation of the current momentum of the vehicle whereas shifting mid-ascent would cause a significant momentum loss.

Another application for this data is to determine whether to disengage the engine while rolling downhill, or to keep it engaged. Disengaging the engine lets the HDV roll further since the gear no longer has to turn the engine, however does require more fuel since diesel has to be injected to maintain idle. Overall, disengaged roll is preferred provided that no additional braking is required, which of course depends on road grade, length of the downhill section and any upcoming road sections. If braking is required, predicting this ahead of time and keeping the engine engaged, utilizing the engine brake, will serve to save the fuel required to keep the engine at idle.

That this type of look-ahead data can be useful for saving fuel is claimed by, among other authors, Hellström et al. [8].

The technology described, and these applications, are already implemented in commercial vehicles by way of preprogrammed map data. A commercial road map, customarily stored in a refined node-based format, forms the foundation upon which such systems operate. Typically, raw data is collected by sensors in special data collection vehicles, and then processed into a node form. Such a format consists of a number of conjoined nodes, each representing a point of the road network. By simplifying, through automatic or manual processes, the data, an unequivocal representation of the road network is obtained. It is upon this data any further analysis is based. Due to its unambiguous nature, a single explicit path can be found with relative ease for the travel to a certain destination.

There are, however, shortcomings to this approach. Though useful, this type of commercial data typically contains large patches of incorrect or missing information. Certain portions of the map could contain erroneous information or could simply be absent. This may be due to inaccessibility of private roads or rapidly changing geography, such as quarries. Another situation for which the aforementioned strategy is insufficient, is off road operation which is common for many types of HDV usage. Yet another reason existing systems are not completely ideal is due to a lack of coverage in certain geographical locations. In certain countries, coverage may be lacking or available only in limited locations. Some situations where knowledge of the road ahead would be the most valuable, such as rough road conditions or mountain roads, may also be the locations where map data is the most likely to be unsatisfactory.

Operation on these types of areas are commonly performed with HDVs. As such, this class of vehicle is especially suited for an alternative approach to the problem.

A proposed solution to augment current inclination-aware navigation to adapt to such conditions is to allow the vehicle to automatically collect road data and build its own map data. This is done by estimating the current road inclination based on input from several sensors, as described by Sahlholm [18], the reason for which being that vehicles currently on the market are not actually equipped with sensors that can produce this result directly.

This would allow the vehicle to store information about any road encountered, and to use this information to its advantage each succeeding pass through that same area.

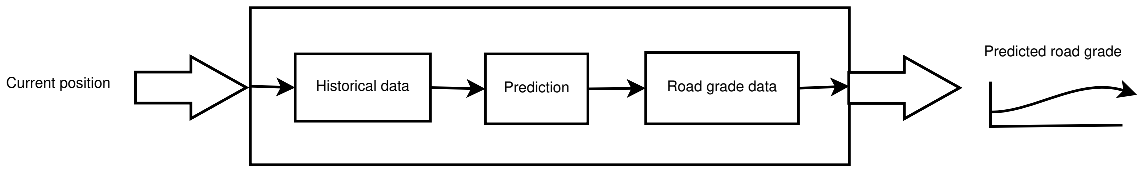

Figure 1.1: The desired system

By feeding the current location, as obtained from a GPS module in the vehicle, to the system, the desired final result is a function that represents the upcoming road inclination for a certain distance ahead, as illustrated in Figure 1.1.

Problem definition

The problem examined in this thesis is the construction of the system in Figure 1.1. This system is to collect positional and road grade estimation data as input data and use it to incrementally construct a topographical map with statistical information about commonly traveled paths. This map will be, simultaneously, used for real-time topographical prediction of the road ahead. In order to achieve this, the route needs to be predicted and the topographical information fetched to predict the upcoming road grade.

Limitations

In order to realize the system mentioned above, several algorithmic solutions and data structure designs are necessary. Furthermore, aside from solving a novel problem, these need to be developed with a certain focus on embedded ECUs. The main limitations are processing, memory, communication and storage constraints of the class of devices. It is certainly possible to install hardware of sufficient capacity to house even a rather unoptimized implementation of such a system, but this is undesirable for several reasons. Firstly, there are budgetary considerations. As HDVs are manufactured in large numbers, cost is to be kept down if possible. Furthermore, the commercial vehicle market is incredibly competitive. Secondly, there is a desire to be able to implement a self-learning inclination prediction system in current hardware already in production. Lastly, any new hardware intended for installation in an automotive system needs to meet strict demands in environmental ruggedness. The equipment will be subject to extreme temperature differences and vibrations, making regular consumer grade equipment unsuitable. This limits the choice of hardware to equipment that is typically simpler in their technological capabilities.

Furthermore, the data bandwidth of the available communication means, i.e. the existing CAN network, is severely limited. It is also shared by critical applications meaning that brevity is of essence when carrying out communication. Another complication is that the length of the desired route prediction, the so-called horizon, is fairly long, as needed by certain applications of the data. This is further explained later on in this thesis.

The CAN message payload is a maximum of 8 bytes, which makes the sending of a horizon a incremental endeavor. It follows, then, that having to discard the current prediction and start all over causes a penalty in terms of performance.

A self-learning route prediction system is useful for mainly these situations:

- Traditional roads not covered by the commercial map being used
- Information unavailable due to private land or land not of particular interest to the general public
- Incorrect road inclination data in commercial map
- Potential high cost of commercial map data

An additional part to be considered is performance in open pit mines and other open areas without strictly defined road structures (falls within bullet point 2). These situations might require a more flexible system than a node system would allow, because the path taken might be subject to larger perturbations between drives. This scenario will be especially considered when evaluating route prediction algorithms to make sure the end result is useful.

The target hardware chosen is based on currently available hardware in production vehicles. The capacity specified is not strict and may be subject to improvement (especially storage). Therefore, a scalable system is desirable, although the main focus is to achieve a robust prediction. If this should require more resources than available, that would be acceptable provided other options have been exhausted.

Methodology

Since the objective of this thesis has a focus on algorithm evaluation, reference points and testing procedures are of importance. Python has been chosen as the environment for carrying out simulations for this purpose, due to its brevity and clarity, which facilitates rapid prototyping. Using this language means that experimentation on different algorithms will be quicker and easier to change than, for example, embedded implementation in C.

The basis for evaluating algorithms and specific road conditions is raw CAN data captures from actual vehicles. This collection of CAN bus recordings, carried out several times over the same route, provides a data set to examine the performance of the chosen algorithms. Measurement noise and natural variations in path are accurately captured. A visualization of the roads covered by this data is viewable in Figure 1.2.

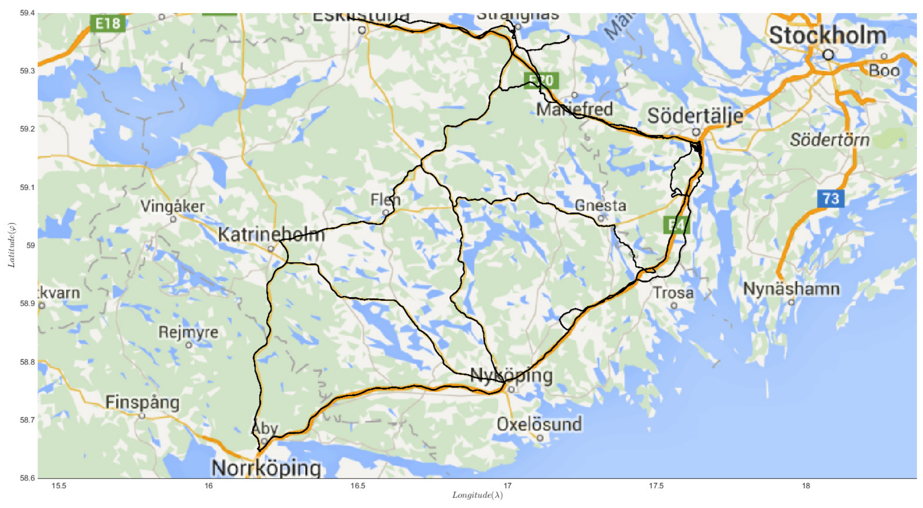

Figure 1.2: A visualization of the road network along which data has been collected. Image: [16]. Map data: Google.

Evaluation is done by simulating driving from several complete traces in order to build a map. Another trace (not recorded in the previous) is then used to represent a unique new travel through the area. This data is completely new to the system, and the prediction builds on the previous data. See Section 4.1 for further details on evaluation methodology.

Delimitations

This thesis does not aim to implement a fully functioning system on an embedded platform, however algorithms and data structures are to be chosen so that they are suitable for such implementation. This means that any code may be implemented in C or any other language as long as a sufficient analysis is carried out to ascertain the suitability of implementation on an embedded target.

The main focus is route prediction, however auxiliary functions such as map data structure and map generation will be delved into with the objective of enabling efficient route prediction. The aim is to end up with a self-contained horizon generation system as an end result, with a functionality as illustrated in Figure 1.1.

Report organization

The report is organized into five chapters.

1. Introduction. This chapter. Contains an overview of the problem and the work carried out as part of this thesis.

2. Background. Details on previous work and explanations of ancillary technologies used for building the specified system.

3. Implementation. In-depth explanations of the implementation of various parts of the system, organized in a logical order such that a narrative for constructing the system is created.

4. Results. Presentation of results in the form of data and charts. Contains some implementation details and discussion in cases where they lay the basis for further investigation of results.

5. Discussion. An overview of the system that is developed within the scope of this thesis. Conclusions and discussion regarding the chosen design and its parameters.

Contributions

This thesis contributes to the field of GIS with a novel method of route prediction through a raster based map, the heat map based route prediction method. In order to use this prediction method, a novel map format is developed that stores n heat maps, each representing a range of possible travel directions.

The novel heat map based route prediction method and its associated storage format is explained in Section 3.4. By using a heat map based map, using the heat as a quality measure is explored in Section 3.6.

Improvements compared to previous solutions in the field include a higher performing linear distance calculation method, shown in Section 3.5, that calculates the average linear travel distance between points in a sliding window. This is important for making sure the horizon is properly aligned to the real world road slope.

Means for controlling the bandwidth usage of the system is implemented, shown in Section 3.8, by controlling which points need to be re-sent and using the discoveries to suggest a new transmission standard. This is valuable when the generated horizons are used as input data in a distributed ECU system interconnected by a bandwidth-constrained CAN bus. Bandwidth performance is exhaustively explored, and a proposal for an approach that works within the current standard is made.

Chapter 2
Background

This chapter presents the reader with an overview of the theoretical background for the problems examined in this thesis. The first section contains some underlying theory that is used as a basis for building the system. Next is presented the technology with which the system is to be realized, and finally an overview of existing map building and route prediction techniques from which inspiration has been drawn.

Theory

In this section, known theory that is used for realizing different parts of the desired system, is presented.

Coordinate mapping

In order to use the system for real-world applications, geographical coordinates are used in system input and output signals. For ease of implementation, however, an internal Cartesian coordinate system is used. This allows for fast and easy data addressing with standard data formats, such as arrays.

The international standard for defining coordinates on the earth as well as the one used by GPS technology is called World Geodetic System 84 (WGS84). A location as expressed in WGS84 consists of a latitude and longitude, which are spherical coordinates and the earth is modeled as an ellipsoid. The coordinates are expressed as an angle from the center of the earth, with latitude 0° at the equator. The range for the latitude coordinate is:

$$\left[-\frac{\pi}{4}, \frac{\pi}{4}\right] \tag{2.1}$$

And for the longitude coordinate:

Φ	Δ_{lat}	Δ_{long}
0º	110.57 km	111.32 km
15º	110.65 km	107.55 km
30º	110.85 km	96.49 km
45º	111.13 km	78.85 km
60º	111.41 km	55.80 km
75º	111.62 km	28.90 km
90º	111.69 km	0.00 km

Table 2.1: The length of one degree of movement at different coordinates

$$\left[-\frac{\pi}{2}, \frac{\pi}{2}\right] \tag{2.2}$$

If one divides the globe with equally spaced pieces in WGS84 coordinates (latitude and longitude), the resulting pieces are not actually equilateral squares, but rather differ in height and width (see Figure 2.1). The width of a one-degree difference Δ_{long} on a sphere of radius a can be expressed as:

$$\Delta_{long} = \frac{\pi}{180} a\, cos\Phi \tag{2.3}$$

It then follows that the width on an ellipsoid would be:

$$\Delta_{long} = \frac{\pi a\, cos\Phi}{180\sqrt{1 - e^2 sin^2\Phi}} \tag{2.4}$$

where e is the eccentricity of the ellipsoid, defined using the equatorial and polar radii by:

$$e = \frac{a^2 - b^2}{a^2} \tag{2.5}$$

The longitude length is given by calculating the Meridian arc. The Meridian arc length from latitude φ (in radians) to the equator is given by:

$$m(\phi) = \int_0^{\phi} M(\phi)d\phi = a(1 - e^2)\int_0^{\phi}(1 - e^2 sin^2\phi)^{-\frac{3}{2}} d\phi \tag{2.6}$$

where M(Φ) is the radius of curvature. It follows, then, that the height of a one-degree latitude difference would be:

$$\Delta_{lat} = \frac{\pi a(1 - e^2)}{180(1 - e^2 sin^2\phi)^{\frac{3}{2}}} \tag{2.7}$$

Evaluating the size of a one-degree difference in latitude and longitude for a few different coordinates yields the result in Table 2.1.

This means that division into quadrilateral pieces as expressed by WGS84 coordinates are not actually equilateral squares, as seen in Figure 2.1. This can present a problem since it is desirable to optimize division size in terms of performance and memory usage, and

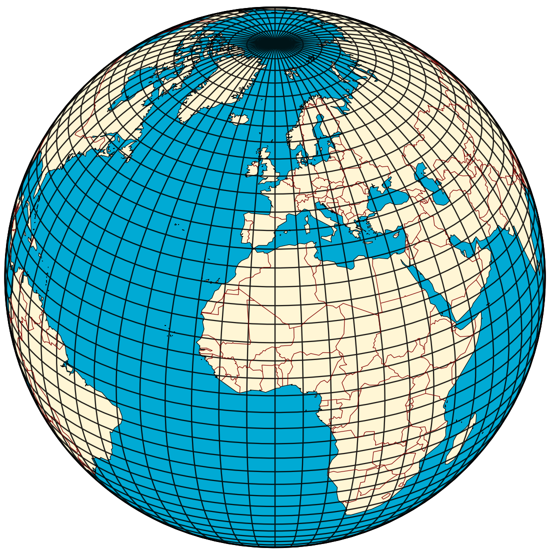

Figure 2.1: The earth divided into quadrilateral pieces as defined by equally spaced WGS84 coordinates. Image: Hellerick on Wikipedia. Creative Commons Attribution-Share Alike 3.0 Unported license.

preferably keep the dimensions equal everywhere. The issue is the greatest with longitude coordinates, and negligible for most intents in the latitude.

For the geographical vicinity of Sweden (since this is the area from which our sample data is collected), this means a quadrilateral piece with an equal span of latitude and longitude expressed in WGS84 standard format, will have a greater height compared to its width. Details of how this is dealt with is presented in Section 3.3.2.

Calculating distances in WGS84

To transform the representation of slope as a function of the data point to the slope as a function of the distance actually traveled, each slope data point is assigned a distance value. This value can be calculated as the accumulated distance traveled when passing through each pixel.

The simplest form of calculating such a distance is to use a linear approximation. Since the entry and exit points are already calculated, finding the distance between these give the distance of linear travel at a fixed direction through each pixel.

These points are converted into a WGS84 coordinate representation and their distance is calculated using the haversine formula. In formula 2.8, the distance between two points on a sphere is denoted d, r is the radius, $\phi_1$and ϕ_2 are the two latitude angles, and λ_1 and λ_2 are the longitude angles.

$$haversin\left(\frac{d}{r}\right) = harversin(\phi_2 - \phi_1) + cos(\phi_1)cos(\phi_2)haversin(\lambda_1 - \lambda_2) \tag{2.8}$$

where the $haversin\ (\phi)$ function is defined as:

$$haversin(\phi) = sin^2\left(\frac{\phi}{2}\right) = \frac{1 - cos(\phi)}{2} \tag{2.9}$$

solving for d yields:

$$d = r\, haversin^{-1}(h) = 2r\, arcsin\left(\sqrt{h}\right) \tag{2.10}$$

where h is equal to:

$$h = haversin\left(\frac{d}{r}\right) \tag{2.11}$$

Since this formula calculates the distance between points on a sphere, it is an approximation compared to the WGS84 representation, which uses an ellipsoid to model the earth. However, the distances sought are very short, compared to the total circumference of the earth, which makes the approximation more accurate.

Quick calculation of arc length

Arc length calculation is necessary to obtain the route length as approximated by fitting a function to the data. In this thesis is explored doing so using polynomials. Here is presented a computationally quick method of calculating the arc length for a polynomial, suitable for embedded implementation.

The arc length of a polynomial $p(x)$ is written as:

$$\int_{x_0}^{x_n} \sqrt{1 + (p'(x))^2} dx \tag{2.12}$$

the derivative of which is trivially obtained from the polynomial.

The integral can be calculated using Simpson's rule, the origin of which is unknown but popularized by and commonly attributed to Simpson [21].

This is a numerical constant-time approximation of an integral:

$$\int_{x_0}^{x_n} f(x)dx \approx \frac{x_n - x_0}{6}\left(f(x_0) + 4f\left(\frac{x_0 + x_n}{2}\right) + f(x_n)\right) \tag{2.13}$$

Splines

A possible approach to calculating the route length is to construct a quadratic spline along the discrete points of the horizon.

A spline is a polynomial interpolation, but it is done in a piecewise fashion, first described by Schoenberg [20]. What this means is that a polynomial is fitted between two points at a time, giving a series of polynomials to interpolate all the points. When using a quadratic polynomial spline, there are three unknowns (see Equation 3.32). This means that using two points to fit such a polynomial leaves one degree of freedom.

To make sure the spline smoothly transitions between the different polynomials, this unknown is eliminated by choosing the polynomial such that its derivative matches that of the previous polynomial. This ensures there are no sharp edges in the spline. Consider two subsequent polynomials $p_i(x)$, $p_{i+1}(x)$ in a spline:

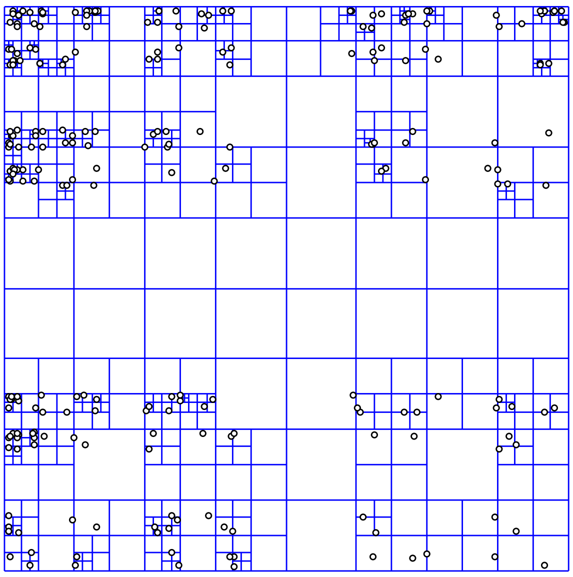

Figure 2.2: Points in a two dimensional space addressed using a quadtree. Image: David Eppstein. Public domain.

$$p_i(x) \mid x \in [x_i, x_{i+1}] \tag{2.14}$$

$$p_{i+1}(x) \mid x \in [x_{i+1}, x_{i+2}] \tag{2.15}$$

$$p_i^{'}(x_{i+1}) = p_{i+1}^{'}(x_i) \tag{2.16}$$

Quadtrees

To address the sparse data created by traveling through a highly limited number of points through a large area (in essence, all of earth), some approach is needed to make the process both computationally quick and efficient, storage-wise.

Quadtrees are a strategy to storing and quickly accessing items at coordinate points. It is an extension of the binary tree with four leaves at each node. It was first named by Finkel and Bentley [6] and although most applications (especially GIS) use quadtrees for two dimensional spaces, it is trivially extensible to any desired dimension.

A two dimensional quadtree, which will be relevant to the implementation in this project, divides the two dimensional plane in four quadrants at each level, making search quick. It is a tree data structure where each node comprises four children. Each level then divides its space into four new quadrants, and this sub division is continued for a number of levels. The bottom most leaves in the tree, as a consequence of a limited number of levels, can theoretically hold any amount of items. Therefore a trade-off is required in choosing the number of levels. One does not want each node to contain too many items, as these need to be searched through by brute force to find the final desired item. On the other hand, too many levels also add additional time to find an item since more level need to be iterated through.

The advantages of this data structure as compared to a two dimensional array is that only the regions that contain data need to be allocated. This is an important point because the self-recorded map data of a HDV is sparse. The quadtree still maintains the main advantage of two dimensional arrays; the ability to find an element quickly (although requiring a few more operations than a two dimensional array). Figure 2.2 visualizes a two dimensional space sparsely populated by points and how they are indexed by a quadtree data structure. In this example, the maximum number of levels is 7, including the single top node. Note that leaves not containing any points are not broken down further into any deeper levels.

A quadtree, in its basic form, is non-discrete in that each node has four bordering sides and any number of non-discrete points may fall within it (this will eventually trigger the creation of deeper levels, provided the maximum limit is not reached). It supports storing any resolution of data.

Technology

This section describes notable technical components that are used in the context of this thesis.

Target platform

The target platform is an embedded ECU for ADAS functionality that is present in production vehicles. The specifications of this ECU defines, roughly, the bounds by which the system should ideally conform. There is, however, some possibility for adjustments to the hardware design before production of the system in question. Especially flash storage can be expanded with relative ease.

This ECU features:

- 800 MHz 32-bit ARM CPU
- 512 MB RAM
- 4 GB flash storage
- Two CAN-buses
- Integrated GPS module

This ECU is shared with other functions, most notably Scania Active Prediction, which is the production look-ahead system that uses commercial map data. The available storage depends on the vehicle configuration, but is at least 1 GiB.

Another important limitation is the bandwidth limitation. In the production system, the CAN bus that connects the ECU housing the ADAS functionality and the ECUs utilizing this data runs at 500 kbps. As is the case with the system resources, this is a shared resource. The way the currently used protocol works (for Scania Active Prediction), the horizon needs to be sent incrementally due to the low bandwidth, not to lock up other communication. This means that having to discard the horizon due to the driver choosing an unexpected route or noise results in a penalty. Therefore, an approach that generates an as robust as possible horizon is needed.

The software side follows the protocol detailed in Durekovic et al. [4]. This is a proprietary and confidential specification but the main take-away relevant to the scope of this thesis is that the receiving client system is flexible in terms of what is possible to do. There is support for receiving multiple horizons or a horizon with splits of different probabilities, in other words a tree where each node represents a split. The receiving system can then make a decision on what to do based on this data.

It is, of course, also possible to perform the selection logic within the supplying system and send the single horizon. This option will be explored in this thesis for the purpose of simulation.

Sample data

To simulate a driving vehicle, some sample data is needed. The data used for this thesis is recorded and processed raw data from the system that would actually be used as system input in the distributed HDV ECU network. The data is serial, sampled at 1 Hz, and each data point consists of, most notably:

- Latitude and longitude pairs
- Current slope estimation
- Time stamps
- Location and slope accuracy status

Since the slope estimation is inaccurate in some situations, such as while shifting gears, and the GPS location is subject to jitter, there are status flags that denote the assumed validity of these signals. A simple handling of the cases where data is deemed inaccurate usually solves this problem sufficiently, but may decrease data resolution in some areas of the map, depending on the approach used.

The data set consists of 34 traces in total, each representing a trip. The data sets were collected with a tractor trailer combination vehicle with an approximate weight of 40 tons. Individual points along the trace may be referred to as the index of the corresponding data point.

Previous work

This thesis has its basis in previous work by Pivén and Ekstrand [16]. These parts are:

- Directional route prediction and associated map format
- Linear entry-exit point distance estimation technique

The road grade estimation used for creating the input data has its basis on work by Sahlholm [18]. The idea for implementing a self-learning map stems from previous internal research at Scania CV AB. The input data used throughout this thesis was collected from Scania HDVs and provided by Scania CV AB.

Map construction

There are several approaches to storing map data, the most widespread of which use a node representation. These are typically used in preprocessed commercial maps and generated from large sets of data collected by special data collection vehicles, or aerial data. Such methods require large amounts of memory and processing power at the time of creation, and are as such unsuitable for use in an embedded context. Furthermore, incremental update and improvement of the map was not a consideration in the development of these methods. There are, however, interesting proposals to node based incremental map building algorithms. Presented here is an overview of the most relevant methods for constructing and using maps for topographical look-ahead.

Kernel Density Estimation

Kernel Density Estimation (KDE), is a method to derive a graph-based road map, independently attributed to Rosenblatt [17] and Parzen [15]. It takes a raster approach to collecting the source data, by dividing the given area into a relatively fine-grained grid mesh. Each location trace is then incorporated into this grid, in any of the available cells. This cell is then given a value based on the input data. There are two approaches to assigning this value; point based or segment based. In a point based approach, the value of each cell represents the number of visits to this cell. A segment based approach, on the other hand, stores the number of traces passing through that particular cell.

The final result, in any case, is a density map from which road center lines can be extracted.

K-means

The K-means clustering method, first named by MacQueen [14] though originally attributed to Steinhaus [22], takes a slightly different approach by dividing the location data into clusters. The algorithm begins by placing clusters in relation to the location points. Location points are then assigned to a cluster based on their proximity to the center of the cluster. Each time a new point is added to a cluster the cluster center is recalculated as the average position of its contained points. This incremental positional change of the clusters may cause certain point to no longer fulfill the criteria of belonging to this particular cluster. Such points are discarded and later assigned to another cluster. This process is iterated until all points belong to some cluster.

Trace merging

The concept of trace merging is to merge traces with each other until a suitable map density is reached. Points are merged if they are sufficiently close to each other, and share roughly the same bearing. This continues until there are no more candidates that fulfill the requirements of a merge. This point is then considered final, and made into a node on the map. Each node gets assigned a weight that increases each time more points are merged into it. By doing so, low-weight nodes can be discarded as likely erroneous. This method is, in contrast to the previous two algorithms, incremental in nature. It is, however, susceptible to errors for high-error data sets as investigated by Biagioni and Eriksson [2], Liu et al. [13].

Incremental trace merging

Hillnertz [10] examines the applicability of the trace merging algorithm for incremental map building and presents an approach for doing so.

For 888 km of road, this data structure uses 21 MiB of storage. Storing 50,000 km of road would require 1182 MiB of storage space. Although possibly satisfactory, it is significantly higher than the raster map structure by Pivén and Ekstrand [16]. Hillnertz [10] does mention that the quoted figure refers to a largely unoptimized system and thus may be subject to improvement. Computational performance is not investigated thoroughly, but it does seem to be slower than a raster map approach. This would need to be evaluated further.

Raster map

This section presents the map format chosen by Pivén and Ekstrand [16]. Their thesis concerns much of the same issues as this one, meaning many of the requirements on a map format are shared.

Rather than choosing a tried and true graph based map format, Pivén and Ekstrand [16] argue that such a map is less suitable for incremental updates under the given constraints, and opt for a raster based approach due to its supposed suitability for the task at hand. The resulting raster map format combines very low storage and working memory requirements, as well as using a minimal amount of processing power.

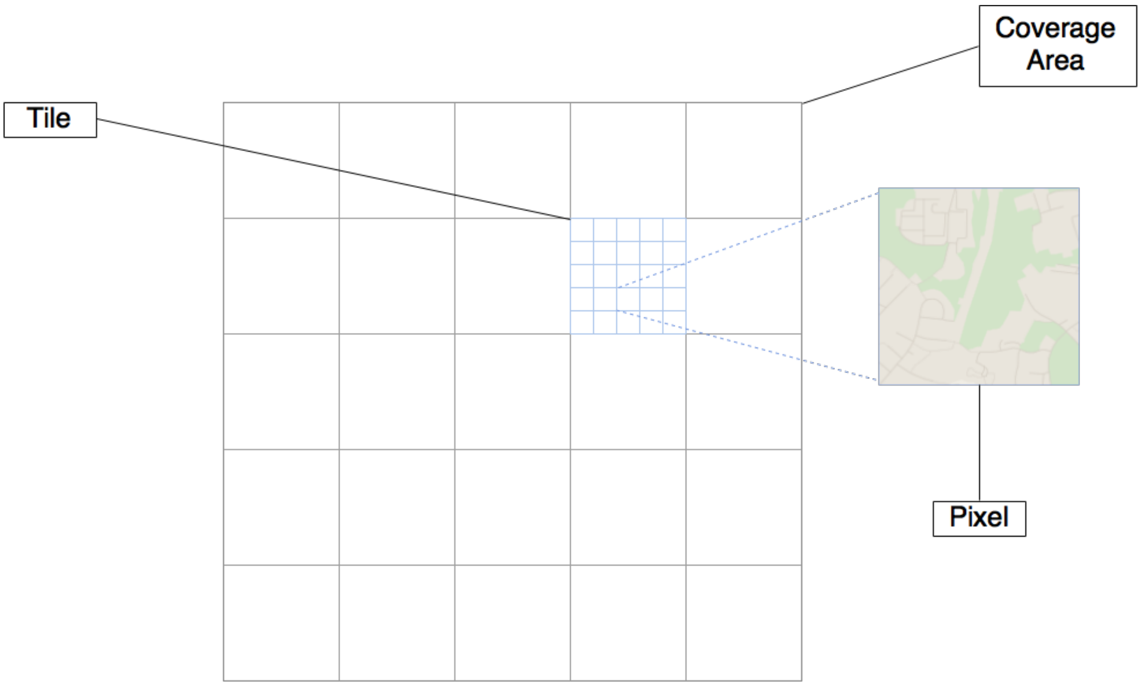

Figure 2.3: The basic idea of the map construction used by Pivén and Ekstrand [16]. Image: [16].

Figure 2.3 shows the basic idea behind the data structure of the map. The coverage area is divided into tiles of a fixed size, which are logical partitions of the map, the purpose of which is to enable memory swapping between RAM and storage. The actual data is stored as pixels, a certain number of which comprise each tile. Different sizes of pixels were experimented with to try and find parameters to give a satisfactory granularity as well as giving sufficiently low-noise results in route prediction and acceptable memory usage. The results of this investigation yields a pixel size of 20 by 20 meters.

The tiles are swapped between working memory and storage as shown in Figure 2.4. Using this strategy, the minimum possible length of a generated horizon is bounded by the worst case scenario of being positioned on the edge of the middle tile with a predicted route perpendicular to the side of the next tile facing the vehicle. This means that the minimum length of a predicted horizon will, assuming road data is available, be the length of the tile side.

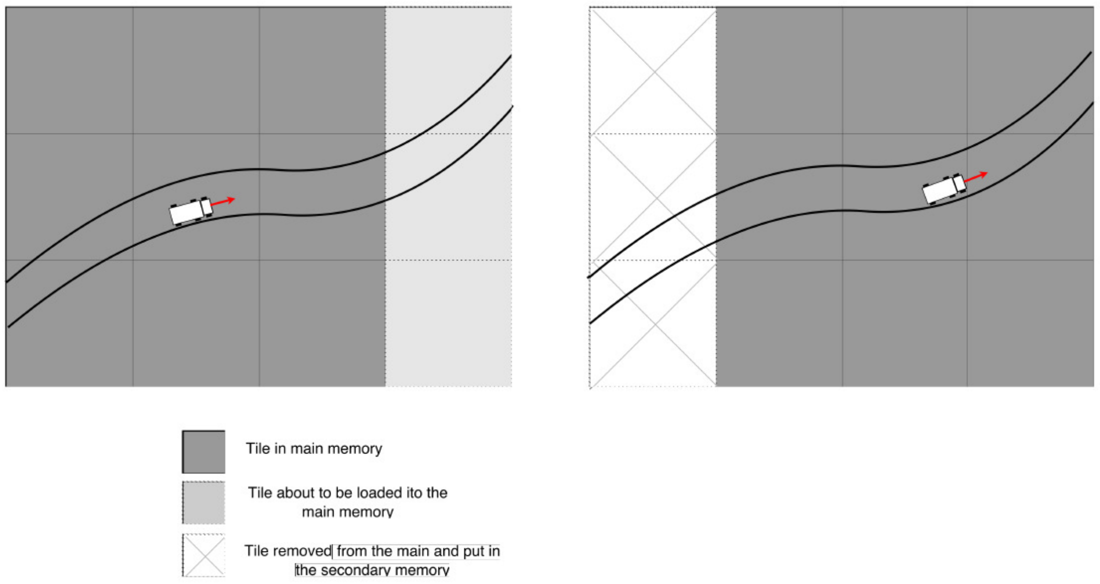
Tile in main memory
Tile about to be loaded ito the main memory
Tile removed from the main and put in the secondary memory

Figure 2.4: Tile swapping as used by Pivén and Ekstrand [16]. Image: [16].

Road grade is stored as four values that represent road inclination in each of the four directions through the pixels. This simplified format means that very little processing is required when updating pixels. Figure 2.5 shows the data structure for an individual pixel.

Tile-based storage

Tile-based storage is used in Pivén and Ekstrand [16] to give some flexibility in storage, and ease of implementation. It can be compared to a quadtree with only one level, containing a high number of nodes. Each node then contains a high number of pixels. Like a quadtree, the correct tile to search for the pixel can be found quickly because it is spatially mapped within the root node. When the correct tile is found, the pixel can be found with similar performance. The design parameter of the data structure is the number of pixels per tile. The main advantage of this approach compared to the naïve approach of storing

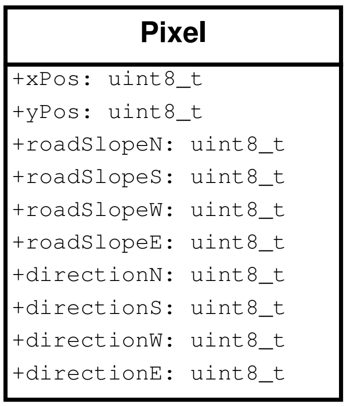

```
Pixel
+xPos: uint8_t
+yPos: uint8_t
+roadSlopeN: uint8_t
+roadSlopeS: uint8_t
+roadSlopeW: uint8_t
+roadSlopeE: uint8_t
+directionN: uint8_t
+directionS: uint8_t
+directionW: uint8_t
+directionE: uint8_t
```

Figure 2.5: Storage format in C struct

the data in an array, is that it accommodates some sparseness in the data set by not having to allocate memory for every single possible pixel (which would be impossible, given the constraints!). However, it is also not the optimal solution since it does have to allocate the entire tile at a time. At the cost of using more memory, performance is very good because finding a pixel only requires a two arithmetic operations (divisions) and a memory access to find the tile, and then another two operations to find the pixel within the tile.

Tiles can be easily swapped between storage and memory to accommodate the limited amount of RAM on the embedded device.

Route prediction

In this subsection are presented existing methods of predicting the most probable route through a road network.

Scania Active Prediction

Scania Active Prediction, as presented in Scania [19], is an implementation of a system that serves a similar purpose to the one examined in this thesis. It uses commercially sourced prerecorded and preprocessed node-based maps that covers most of Europe, but lacks coverage in some other areas. According to Scania [19], fuel savings for highway driving can be expected to be up to 3%. Figure 2.6 offers an intuitive overview of how cruise control can utilize look-ahead data to save fuel.

Route prediction is made from probabilities stored at each node. These values estimate the probability with which the vehicle will choose a certain path for each possible branch in the map. When predicting the route, the branches are already known because of the node format. For each possible branch, the path with the highest probability is chosen and this process is iterated for the desired horizon length. A raster map format, in contrast, has a potential branch at each pixel.

Directional route prediction

Pivén and Ekstrand [16] opt to store all road data in discrete pixels - this includes measured road grade and vehicle pass-through history. This data forms the basis for all further

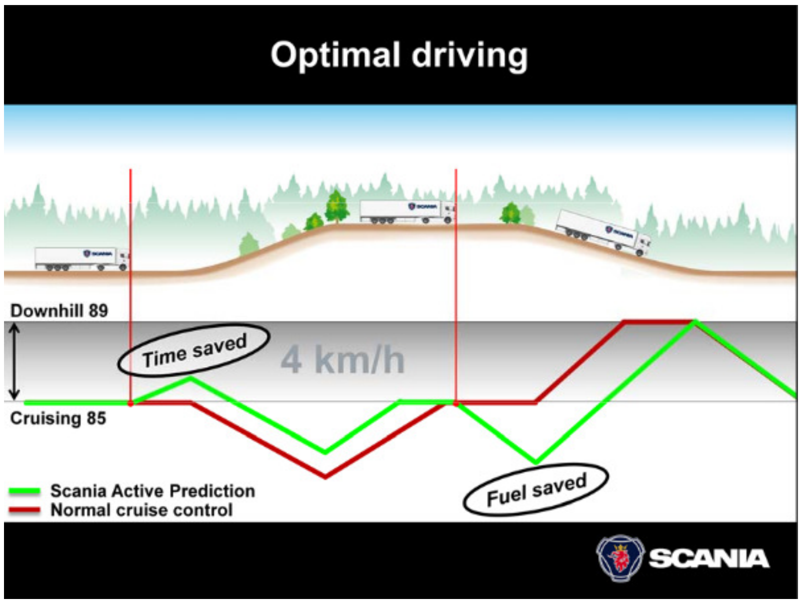

Figure 2.6: Illustration on how cruise control can be optimized for fuel efficiency using look-ahead technology as shown in Scania [19]

operations on the map.

To enable route prediction through this data structure, pixel-by-pixel discrete statistics are examined. The prediction is done by examining which pixel is the likely successor after having visited the current pixel, as given by the current GPS location. This approach thus yields four possible succeeding pixels as shown in Figure 2.7, ignoring the diagonal cases, which are, depending on the implementation, technically not possible.

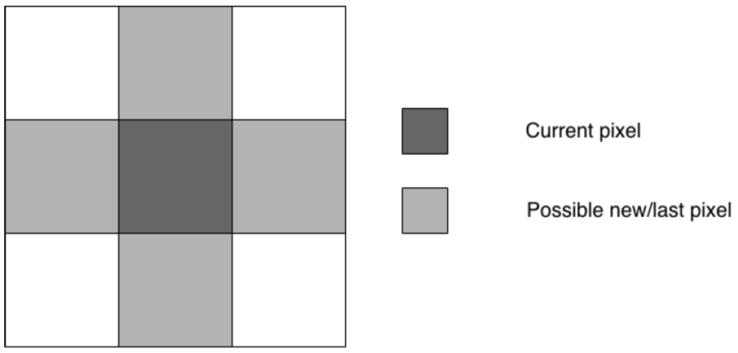

Figure 2.7: Succeeding pixel candidates in route prediction by Pivén and Ekstrand [16]. Image: [16].

To give some granularity to the prediction and allow some support for road crossings and lanes in opposite direction passing through the same squares, a probability is saved for each side of each pixel. The vehicle is said to enter the pixel from south, north, west or east. The entrance side is then used to find the appropriate successor to the current pixel, and this pixel is selected for the next step in the horizon. This is continued on a pixel-per-pixel basis in order to produce a horizon of sufficient length.

The driving statistics through each pixel is updated with each succeeding pass-through, using a weight.

Some noteworthy properties of the approach follow.

+ Memory usage is low at 10 bytes per pixel
+ Relatively simple solution
+ Yields satisfactory results for many cases

- Problems arise when roads fall on the edge of two rows or columns of pixels, and in the worst case scenario the data needs to be duplicated to achieve the same prediction accuracy, because the vehicle would need to pass through both cases and build data for each one separately.
- Highly dependent on pixel size for route prediction. If the pixels are too small, the vehicle might stray into another pixel than the expected one, causing the entire route prediction algorithm to fail and the horizon to be discarded, which is most undesirable for this system as transmission capacity is severely limited.
- Road grade information and driving statistics are coupled, while the two might benefit from different parameters.
- Road grade granularity, route prediction accuracy and memory performance are all coupled. Some trade-off needs to be chosen.

Horizon length

In an article by Hellström et al. [9], the optimal length of a horizon, with regards to fuel economy, is examined. Cost of operation of a HDV is modeled and this model is used to test different horizon length for several routes. The results show that a horizon length of 2.5 km is sufficient for a near-optimal prediction in terms of fuel savings for virtually all real-world cases.

Chapter 3
Implementation

This chapter presents explanations of the specific implementations made for the purpose of this thesis. First is presented an overview of how the two parts (map building and route prediction) of the system work. Then follows an explanation of how the map building works in detail, after which an explanation of how the route prediction works. Especially interesting (in a performance perspective) implementation details are presented in their own sections.

Overview

The system can be divided into two logical parts that run in series.

1. Incremental map building. The map is constructed using recorded sensor data for each new data point sent to the input.
2. Horizon generation. The system predicts the upcoming road slope in real time (a period of one second was used in simulations).

Figure 3.1 shows an overview of the map building process. The inputs to this part are the current GPS position and the current estimated road slope. The system uses the current heading to find the correct heat map and the GPS position to find the corresponding pixel in the map. If the pixel does not exist, it is created at this point (only pixels with data are stored). The slope value is then recorded and stored, and the pixel heat is increased.

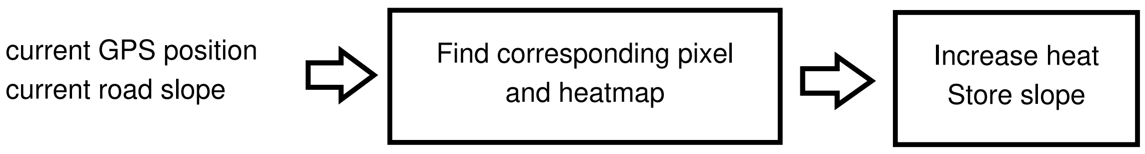

Figure 3.1: The map building part of the system

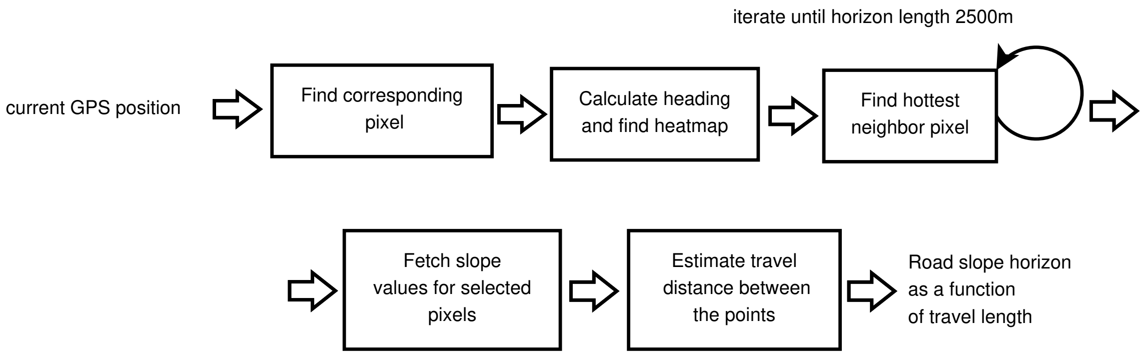
iterate until horizon length 2500m
current GPS position
Find corresponding pixel
Calculate heading and find heatmap
Find hottest neighbor pixel
Fetch slope values for selected pixels
Estimate travel distance between the points
Road slope horizon as a function of travel length

Figure 3.2: The horizon generating part of the system

Figure 3.2 shows an overview of the horizon generation process. The current GPS position is used to find the corresponding pixel. The current heading is calculated by comparing the position to the previously recorded GPS position, and the heading is used to find the corresponding heat map. The neighboring pixels in this heat map are examined to find the hottest pixel, as defined by their heat value. That pixel is then selected and the step is iterated for the desired horizon length. After this step is done, the series of pixels are examined to extract their road slope values. Finally, the travel distance between each point in the horizon is estimated to generate a final road slope as a function of travel length.

Re-implementation of previous work

This section presents the reader with information of re-implementation of previous work for the purpose of comparison and parameter tweaking in the simulator developed for obtaining the results in this thesis.

Discrete road grade format

This road grade format is re-implemented from Pivén and Ekstrand [16]. In their thesis, this format is used for storing road grade data in a pixel.

The discrete approach simply uses the recorded value and weighs it against the previous stored value with some inertial parameter α.

$$\Phi(n+1) = (1-\alpha)\Phi(n) + \alpha\Phi(n-1) \tag{3.1}$$

where α is a constant. While not yielding the most accurate average value, this method requires a low amount of storage and processing power as only one value per direction need be stored.

For the directional route prediction algorithm with four possible directions, this means that there are also four slope values stored for each pixel. An advantage of this approach is the low computational complexity. Each pass through a pixel requires only a multiplication and an addition to be performed to update the value, and recalling the value when predicting the upcoming road grade is simply a matter of fetching one of the stored values.

For the heat map based algorithm, the road grade is similarly stored as one value per directional heat map. This allows some flexibility in recall. Depending on the number of directional heat maps being used, values for the same pixel in several heat maps may be weighed together based on the amount of available data. This can improve performance in situations with few data points without sacrificing resolution when many data points are available.

Directional route prediction

This per-pixel directional route prediction has its basis in the algorithm described in Pivén and Ekstrand [16]. In order to collect data on the performance of this algorithm and easily try out adjustments, it is re-implemented. This implementation calculates the most probable next pixel for each pixel in the horizon based on historical direction through the pixel, when entered through one of the four possible edges. The process is iterated for the desired prediction length, thus producing a string of pixels to pass through. Each pixel is divided into four areas; possible entrance from the north, east, south or west. For each possible entrance direction, the most likely exit direction is stored, as is the road slope recorded in that particular direction. Both these variables are stored as a rolling average of each recorded data point, as described in Equation 3.1.

While not yielding the most accurate average value, this method requires a low amount of storage and processing power as only a single value need be stored. For each point in the GPS trace, the pixel which contains the current coordinate is found and its northern, eastern, southern or western parameter pair is updated according to the formula above, inferring the current bearing of the vehicle by calculating the difference between the previous coordinate pair and the one before that. The most current position is used to infer the subsequent heading. Thus, three positional data points are used to update a single pixel.

To generate the horizon, the current GPS coordinate is compared to the previous one. This gives a current bearing and position. The latest position is converted into a decimal Cartesian coordinate. By truncating the value into an integer, the current pixel in the map is found. Subtracting the pixel position from the actual non-truncated Cartesian coordinates yields the position of the vehicle inside the pixel itself, in the range $[0, 1]$. This internal position is used as a starting point for trigonometric calculation in the route prediction algorithm.

Finding entry and exit points

This method is a variation on the implementation used by Pivén and Ekstrand [16]. To determine the exit side from a pixel and entry side in the subsequent pixel, and to find the most plausible travel as determined by the method, exit and entry points (see Figure 3.3) need to be found.

In order to find the most probable subsequent pixel, a linear extrapolation from the internal point in the current bearing is drawn. This is done by forming an expression of the line:

$$k = \frac{1}{tan(\gamma)} \tag{3.2}$$

$$m = y_0 - k * x_0 | x, y \in [0, 1] \tag{3.3}$$

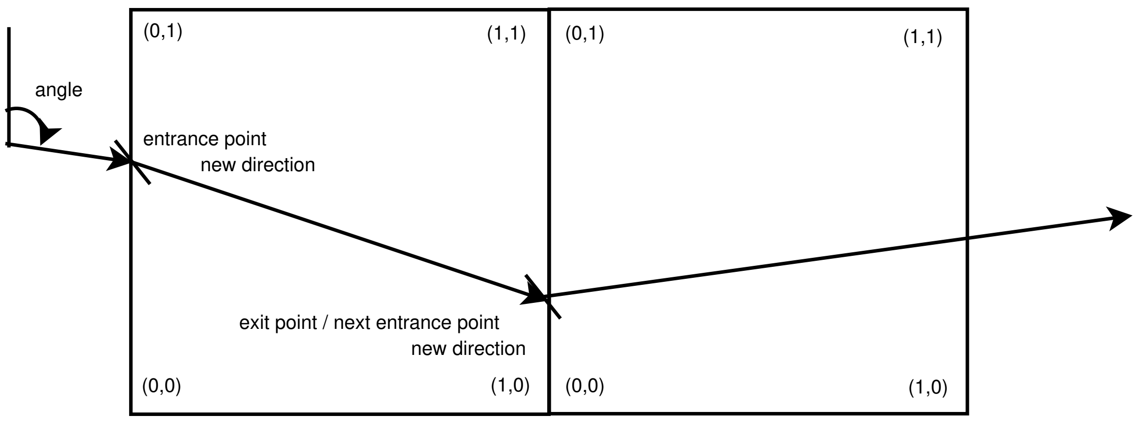

Figure 3.3: Entrance and exit points within pixels of the map and their positions expressed in relative in-pixel coordinates

Algorithm 3.1 Transforming the exit point into the entrance point of the subsequent pixel

```
if x == 0:
    x = 1
elif x == 1:
    x = 0
elif y == 0:
    y = 1
else:
    y = 0
```

and using a first degree polynomial:

$$y = kx + m \tag{3.4}$$

$$x = \frac{y - m}{k} \tag{3.5}$$

to find the possible exit points for the assumed travel through the pixel. The exit points are characterized by being points on the border of the pixel, and thus must fulfill the following condition, which gives four possible points.

$$x \vee y \subseteq \{0, 1\} \tag{3.6}$$

The sought after point can be found by virtue of not being outside the pixel borders, as well as conforming to the correct direction.

Once the exit point is found, the next pixel is known because it will be the pixel sharing the same border as the one of the exit point. This pixel is then selected as the hypothetical next pixel to continue calculating the horizon from the previous pixel in the horizon.

In order to yield a correct result from now on, the entrance point of the pixel is used as a starting point from which the route continues in the predicted direction through that particular pixel. Using the previous exit point, the entrance point is found using Algorithm 3.1.

The system now works satisfactorily when running the same GPS trace twice, which is to be expected since all passed coordinates will have data recorded. However, when running a new GPS trace (which would be the case in real-life usage), an issue arises where some pixels passed will be devoid of data because of never having been passed before. To alleviate this, a simple look-around algorithm is deployed. If a pixel is missing data, its neighbors along the same direction are checked. If these are also empty, the current heading is assumed and a line is extrapolated in the hope of finding upcoming pixels that do contain data.

The entry and exit points are used to approximate travel through a pixel as a linear segment. Route length is estimated by taking the sum of each of these linear segments.

Map building

This section explains the incremental building and storage of the topographical and statistical map and its format. The resulting system corresponds to Figure 3.1.

Data point interpolation

The method of obtaining the raw data, as described by Sahlholm [18], is based on estimation from several input signals and unusable during certain circumstances such as in between gear changes. This means that some gaps in the stream of input data are to be expected, resulting in “skipped” pixels, which will not be updated with historical route data. In order to rectify this, a line interpolation algorithm is utilized to calculate which pixels were likely passed between two consecutive recorded points, and their data is updated accordingly.

The problem can be reduced to drawing a straight line between two points, on a mesh grid. This is done using the Bresenham [3] line drawing algorithm, which is commonly used in computer graphics implementations for drawing non-anti aliased lines with high performance. Because a line can be expressed as movement along the y axis and x axis on a two dimensional plane, if we define movement along the x axis to be constant, the line then becomes a function of y. The line can be expressed as:

$$y = \frac{y_1 - y_0}{x_1 - x_0}(x - x_0) + y_0 \tag{3.7}$$

for the starting point (x_0, y_0) and end point (x_1, y_1).

When drawing the pixelated line, each pixel will contain a certain error from the actual line. This error is calculated and the pixels that minimize the value are filled in. If an arbitrary line is approximated as a horizontal line, the error will increase linearly with the following value at each point:

$$\Delta_{error} = \left|\frac{\Delta_y}{\Delta_x}\right| \tag{3.8}$$

The algorithm starts by drawing this horizontal line and accumulating the error. When the error reaches 0.5, the y coordinate is either increased or decreased depending on the direction of the line. This causes the cumulative (signed) error to decrease by one. By iteration, the entire line is drawn.

Algorithm 3.2 Python code for a simplified Bresenham line drawing algorithm

```
for x in range(x0, x1+1):                 1
        points.append((x,y))              2
        error += deltaerr                 3
        if error > 0.5:                   4
                y += 1                    5
                points.append((x,y))      6
                error -= 1                7
```

Note that the error fraction Δ_{error} can be multiplied by an arbitrary scalar as long as the condition for switching the y coordinate is multiplied by the same constant. Doing so means that implementing the Bresenham algorithm without floating point logic is easy. This makes the algorithm quick on a small microprocessor and highly suited for implementation on an embedded ECU. Furthermore, the algorithm only has to run on each sample (1 Hz in this case) and only if the speed is such that pixels are skipped.

In order to ensure compatibility with a raster map that disallows diagonal movement, a trivial modification to the algorithm makes sure that selected points are always horizontally or vertically adjacent. In the code in Algorithm 3.2, this modification consists of the addition of program line (6). For the heat map based map, diagonal movement is allowed.

Figure 3.4 and 3.5 show the difference between a naïve and an interpolated approach.

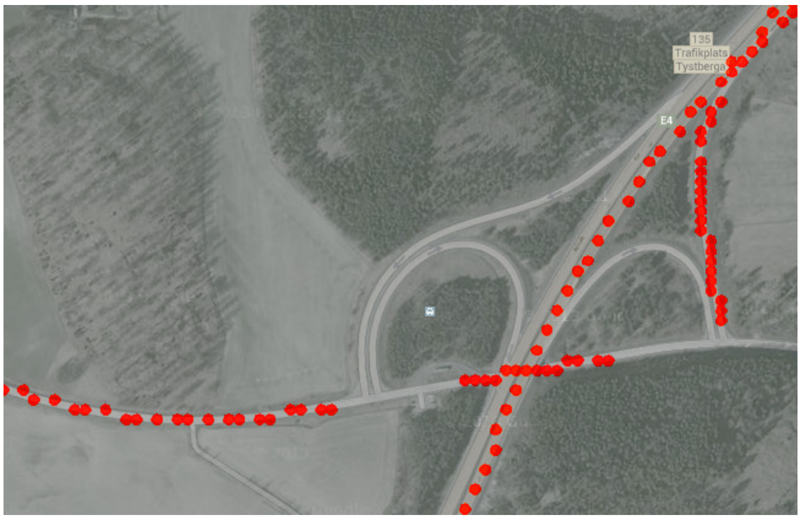

Figure 3.4: A piece of a map constructed using each discrete GPS sample only. Map data: Google, Lantmäteriet/Metria.

Correcting pixel size

As mentioned in the Background chapter, dividing the earth into Cartesian coordinates evenly along the longitude results in vastly different horizontal pixel sizes, meaning pixels in for example Scandinavia will be smaller than those at the equator. For consistent performance, equal pixel sizes are desired. This is accomplished by a longitude correction factor. The number of pixels is calculated as:

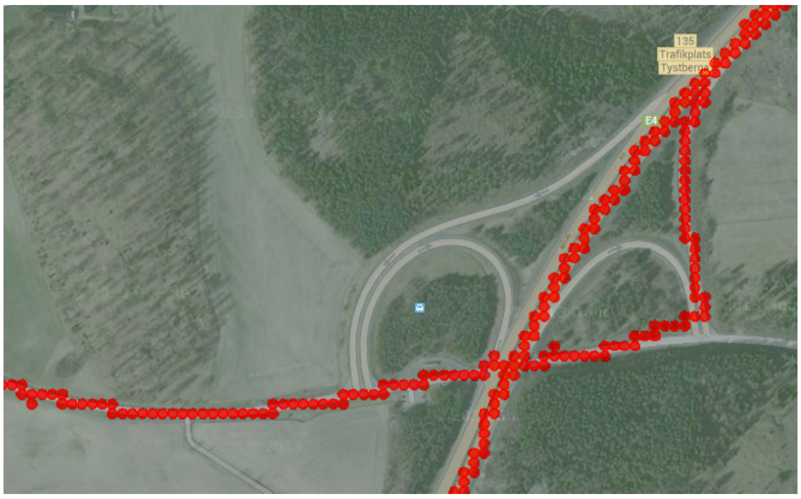

Figure 3.5: The same map portion created from a single trace, with Bresenham interpolation. Map data: Google, Lantmäteriet/Metria.

$$n_{long} = max\left(\delta\,\frac{circumference_{equatorial}}{size_{pixel}}, 1\right) \tag{3.9}$$

for a correction factor δ. The correction factor uses a spherical approximation of the earth, with a cross-sectional circle:

$$x^2 + y^2 = r^2, \; r = 1 \tag{3.10}$$

setting $r = 1$ means that the pixel size, $size_{pixel}$, will approximately hold everywhere in our coordinate system. This means that:

$$\delta = y = \sqrt{1 - x^2} \tag{3.11}$$

$$x = \frac{|latitude|}{90} \tag{3.12}$$

$$-90 \leq latitude \leq 90 \tag{3.13}$$

Since the latitude ranges 90° in each direction as in Equation 3.13, assigning x as in Equation 3.12 means that x will range from 0 at the poles of the earth, to 1 at the equator. It follows, then, that the pixel size (Equation 3.9) will be corrected by having fewer pixels closer to the poles.

Precisely at the poles of the earth, the number of latitudinal pixels would be zero. This is avoided by setting the number of pixels to be at least one.

Planar road grade format

The planar approach to road grade storage stores the road grade in a pixel as a plane, as seen in Figure 3.6. Each pixel is initialized with a neutral road grade of 0° in all directions, giving a plane with the normal vector:

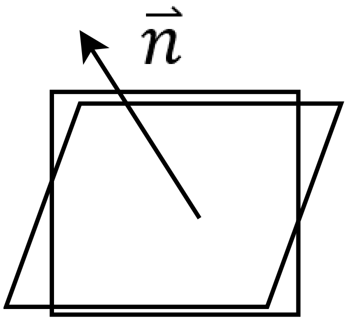

Figure 3.6: Illustration of using a planar approach for storing the road grade within a pixel

$$\vec{n} = [0, 0, 1] \tag{3.14}$$

If we define a point:

$$p = \left(\frac{1}{2}, \frac{1}{2}, 0\right) \tag{3.15}$$

that is in the center of the pixel (defined with dimensions $(1, 1)$), it, together with the normal vector, defines the plane that represents the road grade in the pixel. If the point is constant, only the three components of the normal vector need to be stored. Furthermore, by using a normalized vector, one of the points can be omitted as it can be calculated from the other two points at run time.

The advantage of this approach is mainly in data consistency. Rather than saving many grade values, which may be internally inconsistent, a plane will at all times describe an unambiguous slope in three dimensions. It will also represent reality more accurately, and make the most out of the limited input data. Two passes through the pixel in two different directions is sufficient to build a plane that perfectly represents reality within the given limitations (i.e. assumed linear road grade within each pixel), whereas storing four or more directional road grades requires each direction to be passed through at least once in order to gather enough data. The drawback, of course, is more intense computational requirements.

Each pass through the pixel will update the plane so as to contain the current trajectory, in three dimensions. In other words, fitting the plane to two points $a_{entrance}$ and a_{exit}:

$$a_{entrance}, a_{exit} \in \mathbb{R}^3 \tag{3.16}$$

constructed from the entrance and exit points, respectively.

$$p_{entrance}, p_{exit} \in \mathbb{R}^2 \tag{3.17}$$

Two arbitrary points $p_{entrance}$and p_{exit}, are transformed the following way:

$$p_i = (x_i, y_i) \tag{3.18}$$

$$a = (x_i, y_i, \pm\frac{slope}{2}) \tag{3.19}$$

So that the slope will be the different between the z-values of the 3-dimensional entrance and exit point.

This is an under-determined system which means that the plane will inherently retain some previous data at each pass through.

Another advantage is granularity. The planar approach will not truncate different directions into one of n possible directions, but will allow a more accurate approximation of the road grade when passing through the pixel at a slightly different angle than the previous time. Although this improved accuracy will, in most cases, be small for reasonably small pixels.

In order to determine the new plane after a new pass through, after $a_{entrance}$and a_{exit}have been calculated, the new plane is found by calculating its new normal vector. This is done by first finding the vector of the two recorded points:

$$\vec{v} = a_{exit} - a_{entrance} \tag{3.20}$$

A third vector:

$$\vec{u} \mid \vec{u} \perp \vec{v},\ \vec{u} \perp \vec{n} \tag{3.21}$$

is constructed by taking the cross product:

$$\vec{u} = \vec{n} \times \vec{v} \tag{3.22}$$

This gives the new normal vector as:

$$\vec{n} = \vec{u} \times \vec{v} \tag{3.23}$$

which together with the previously defined point p gives the new plane that passes through the desired points.

To reverse the process and obtain the slope, the two dimensional entrance and exit points to the pixel are calculated. Using the following description of a generic plane, and its relation to the normal vector:

$$ax + by + cz + d = 0 \tag{3.24}$$

$$\vec{n} = [a, b, c] \tag{3.25}$$

$$a, b, c \in \mathbb{R} \tag{3.26}$$

The x and y coordinates of each point is plugged into the plane description and the z value is calculated. The value of the scalar d is calculated using the fixed point defined previously. The z value gives the distance from the plane to the imagined point on the two dimensional pixel. Adding the z values of both border points in the current direction gives the slope in that direction.

Decoupled road grade data

Since there are pixel size trade-offs between accuracy, sparseness and the number of probable paths, the ideal pixel size for predicting the route might not necessarily be the ideal size for storing the road grade data. Therefore, a decoupled road grade map is implemented that makes use of an incremental trace merging approach, as described in Section 2.3.1. This is implemented as an alternative to storing the road grade on a per-pixel basis and an evaluation is presented in Section 4.6.

Slope values are stored in a separate map, without specific pixel sizes. Instead, they are stored as nodes and the closest node for any given coordinate is the road grade at that point. When another measurement is performed, it is merged into an existing node if the coordinate is within a certain vicinity of an existing node, and the road grade difference is lower than a certain threshold. When nodes are merged, their road grade values are averaged together, as are their coordinates. This means the nodes dynamically move around as they are merged into each other.

If the aforementioned conditions are not met, a new node is inserted into the map. The idea is to store road grade information on an as-needed basis, allowing for more data in regions with varying road grade. This approach may be used with either the discrete road grade format, or the planar road grade format.

Three parameters govern the behavior of the algorithm:

- lim_{diff} is the maximum allowed road grade difference between nodes. If the absolute difference is smaller than this value, they are eligible for merging.
- $lim_{dist}$is the maximum allowed distance for merging nodes. If the distance between them is smaller than this value, they are eligible for merging.
- $min_{dist}$is the minimum distance between any two nodes. If the distance between them is smaller than this value, they are unconditionally merged. The intent of this parameter is to counteract noisy data and avoid populating a very small area with road grade values of wildly different values, as this most likely indicates measurement error. Instead, by merging those nodes, the measurement become more accurate.

Heat map based route prediction

A heat map (first named in a patent by Kinney [11]) is a raster matrix that stores a frequency value ("heat") for each element. It is typically used for visualization of data sets, particularly to map frequency of a certain occurrence or prevalence in a two dimensional plane. The name is derived from the common display of such heat maps as colored overlays ranging from blue (cold) to red (hot), indicating a range of relative frequency. For a route finding application, each time the pixel is passed through, this value in incremented. The heat, then, represents the probability of travel for that particular pixel in the map.

A novel approach to route prediction based on the historical frequency of travel through each pixel is developed by constructing a number of heat maps, each representing a different range of possible vehicle headings. When the vehicle travels through a pixel, its

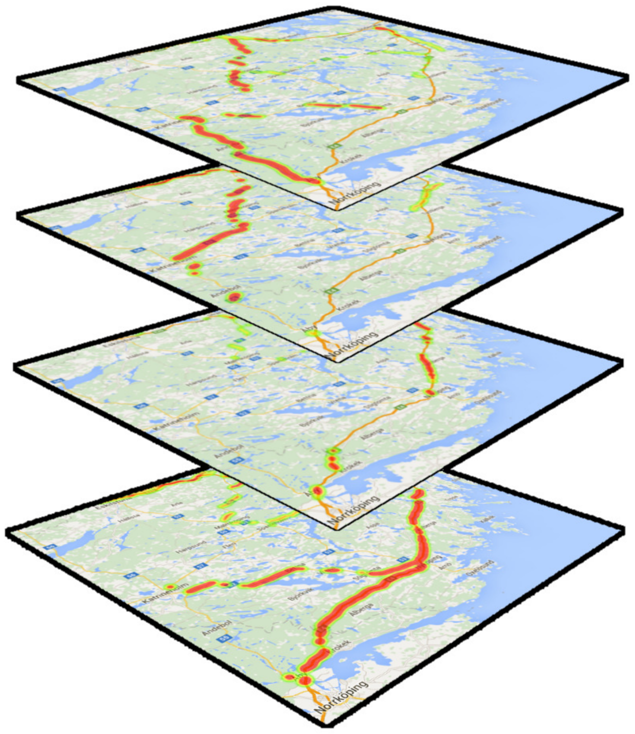

Figure 3.7: A four component directional heat map. Map data: Google. Top to bottom: heading south, west, north and east.

heading is calculated and used to increase the heat in the heat map most closely corresponding to that direction. The number of such directional heat maps is adjustable. A graphical representation of such a map is shown in Figure 3.7.

Recording

Figure 3.8 shows how the pixels are updated. When the vehicle passes through a pixel (when a data point is recorded), the corresponding heat map among the *n* directional heat maps is found by calculating the heading of the two previous points (the previous recorded point and the one before that). Note that the spacing of the previous points, from which the direction is calculated, affects the course stability in routes predicted in the resulting map. The directional heat map most closely matching this direction is selected and the heat value for this pixel is increased in the chosen heat map. Figure 3.8 shows, for a four directional heat map, pixels that were updated in north bound direction (orange), west bound (blue, diagonally striped fill) and south bound direction (green, dotted fill). Note that the heading is calculated with some delay, as shown by the north bound pixels.

The directional approach means that complex situation such as crossing paths will not interfere, while still allowing complex path taking patterns and prediction. A variety of parameters allow for tuning of performance in such situations.

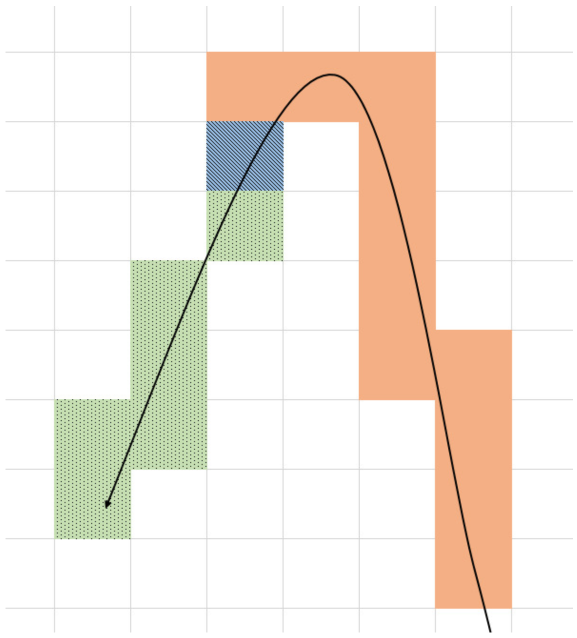

Figure 3.8: Updating directional heat map according to travel direction

Predicting

When the prediction is made, the corresponding directional heat map is used to calculate the next likely pixel. First, the correct heat map is determined by calculating the current heading and assigning it to one of the predefined directions, depending on the number of directions in the directional heat map.

For each possible next pixel candidate, the heat is computed as such:

$$heat_{candidate} = heat_{current\_direction}\left(\frac{\angle[\vec{v}_{current}, \vec{v}_{candidate}]}{\pi} + \alpha\right) \tag{3.27}$$

where $\vec{v}_{current}$ is the current direction vector and $\vec{v}_{candidate}$ is a vector drawn between the current pixel and the candidate pixel as in Equation 3.28. Take $\angle[\vec{v}_{current}, \vec{v}_{candidate}]$ as the closest absolute angle between the vectors, such that Equation 3.29 holds.

$$\vec{v}_{candidate} = pixel_{current} - pixel_{proposed} \tag{3.28}$$

$$0 \leq \angle[\vec{v}_{current}, \vec{v}_{candidate}] \leq \pi \tag{3.29}$$

α is a parameter that sets a minimum multiplier. This means the heat of the direction corresponding to the current heading will be multiplied by a factor:

$$\alpha \leq \left(\frac{\angle[\vec{v}_{current}, \vec{v}_{candidate}]}{\pi} + \alpha\right) \leq \alpha + 1 \tag{3.30}$$

the purpose of which is to give priority to a prediction that continues the current heading approximately, which is almost always true at a pixel level.

The current direction is calculated as a the angle between the current pixel and a pixel n places back (sliding window). This is kept track of using a queue. The distance n between which the angle is calculated determines the granularity due to aliasing, and also willingness to change direction.

When the number of directions is set to, for example, four, the result is four separate heat maps, one for each direction, as seen in Figure 3.9. Each heat map represents the frequency through which each pixel is traveled, on the condition that the direction falls within the threshold. When doing a prediction, one of the four heat maps is chosen depending on the current direction, and used to calculate the probability of the next pixel.

Figure 3.9 shows, starting in the upper left corner, the heat map for direction south, west, north and east. Travel in the specified direction will be evident as more heat (red) in the portions of the map where travel in that direction is more commonplace.

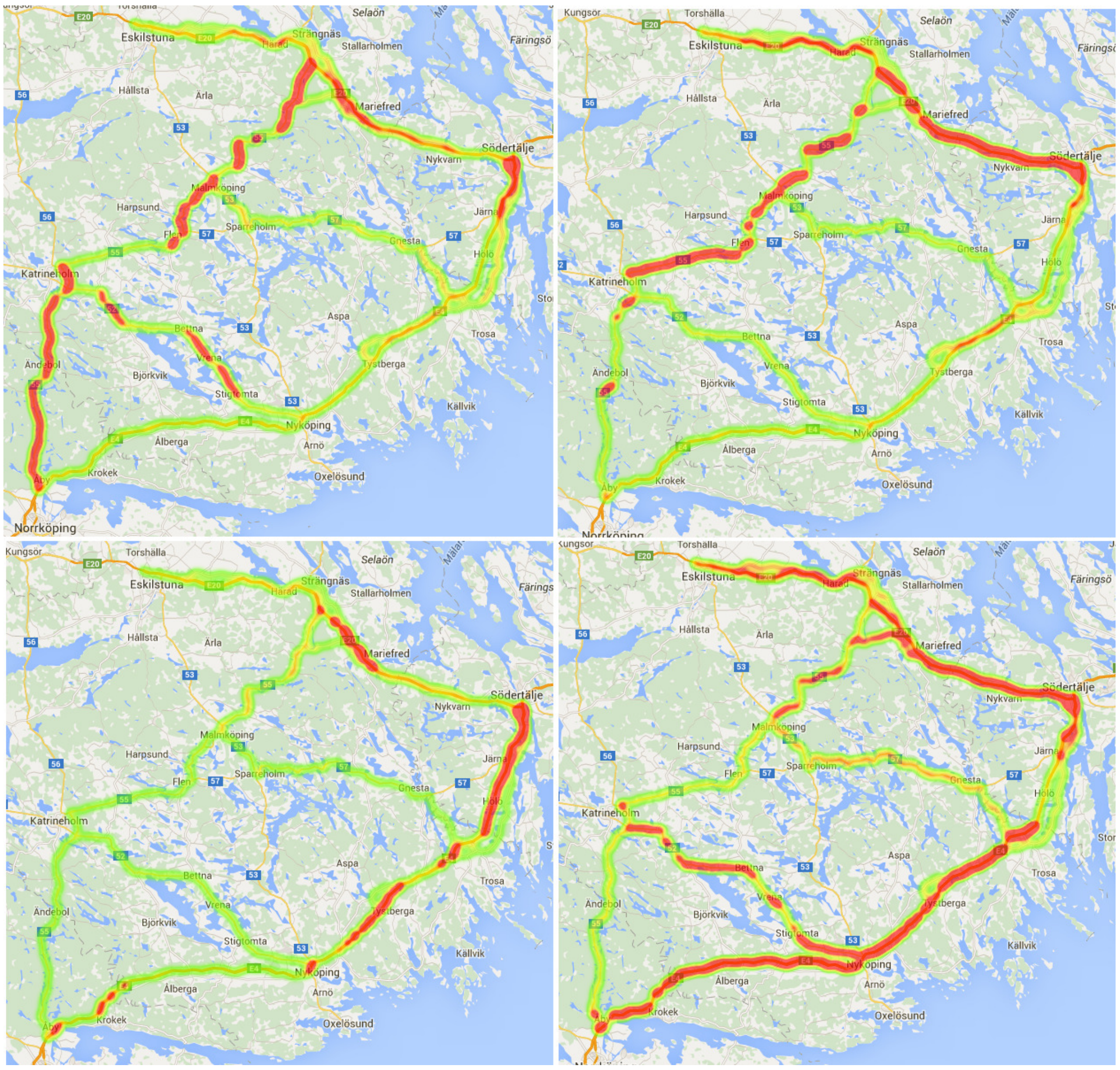

Figure 3.9: The four components of a directional heat map with four directions. Map data: Google. Left to right: heading south, west, north and east

Figure 3.10 illustrates the composition of the map system and how it is accessed to produce a route prediction. In the figure, one heat map is selected depending on the travel direction and the pixel heat values of that heat map examined to find the most likely succeeding pixel for travel.

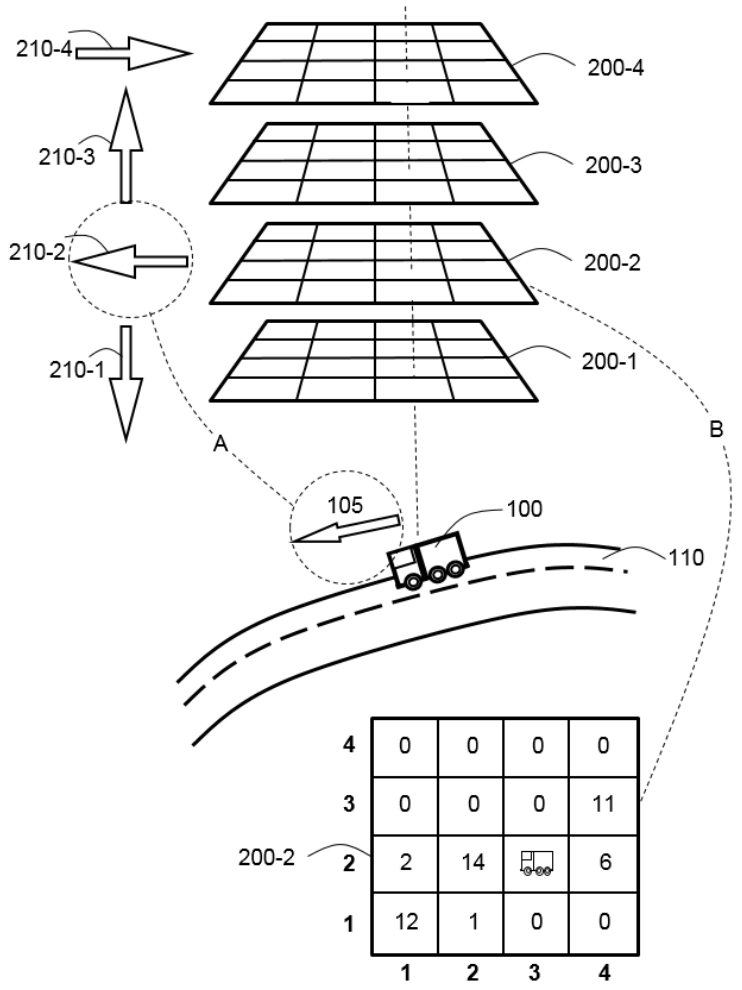

Figure 3.10: Selecting one of several heat maps according to travel direction, and using heat values for predicting the route. Image: patent figure from patent by Fabian [5]

Even though the heat maps are directional, it may sometimes happen that the most likely route is one that loops around. Sometimes, this may be the desired behavior such as low-speed situations in quarries and other tight navigational spots. At other times, however, this may be unreasonable due to travel at highway speeds or simply unlikely depending on the road conditions. To deal with this problem, a parameter is introduced to limit the maximum allowed number of travels through the same pixel. By limiting this value, endless loops are minimized to essentially a single round-trip through two pixels, and then continuation in the correct direction. This essentially amounts to a work-around but it does eliminate problematic situations in a reasonable way, error-wise. When considering the complete horizon, the remaining temporal error produced by such a loop is in most cases negligible.

Algorithm 3.3 Local aging through scalar multiplication

```
let heat = heat in direction
if heat is at max bound then
        for demote in heat_values_in_pixel do
                demote = demote * 0.95
        end
else
        heat = heat + 1
endif
```

Algorithm 3.4 Local aging through subtraction

```
let heat = heat in direction
if heat is at max bound then
        for demote in heat_values_in_pixel do
                demote = demote - 1
        end
else
        heat = heat + 1
endif
```

Aging

Aging is the process of lowering the heat at each pixel through some method, the purpose of which is to keep all values from overflowing their data type. If the value was simply capped, the steady state would be a map of equally hot pixels everywhere, which would defeat the purpose of such a map. Therefore, some type of aging is needed to preserve the data.

Several approaches are possible. One might used a timer to globally decrease the heat after a pixel has not been passed through in a certain time, or decrease the heat for border pixels along the way. The problem with the first proposal is it requires a lengthy processing step. It is perhaps conceivable to perform such a task when the vehicle is idle.

A simpler and more realistic solution to this problem is to perform the aging at a single pixel when it is passed through. To do this, the heat of the current direction is calculated. If it is at the maximum bound of its data type, the other heat values in the pixel can be scaled back by some scalar as shown in Algorithm 3.3. This keeps the proportions intact, and prevents overflow in a manner with very low computational overhead. A conditional statement is added, which is bypassed the majority of time (depending on the scalar chosen and data type). Another possibility is to subtract all heat values in the pixel except the current one, as per Algorithm 3.4.

Loops

To eliminate U-turns of the highway, endless loops and other problems, the number of allowed visits to each pixel in a single horizon is limited.

The parameter governing the amount of visits per pixel allowed in each horizon has a great impact on the predicted route. The reason for this is because this setting governs

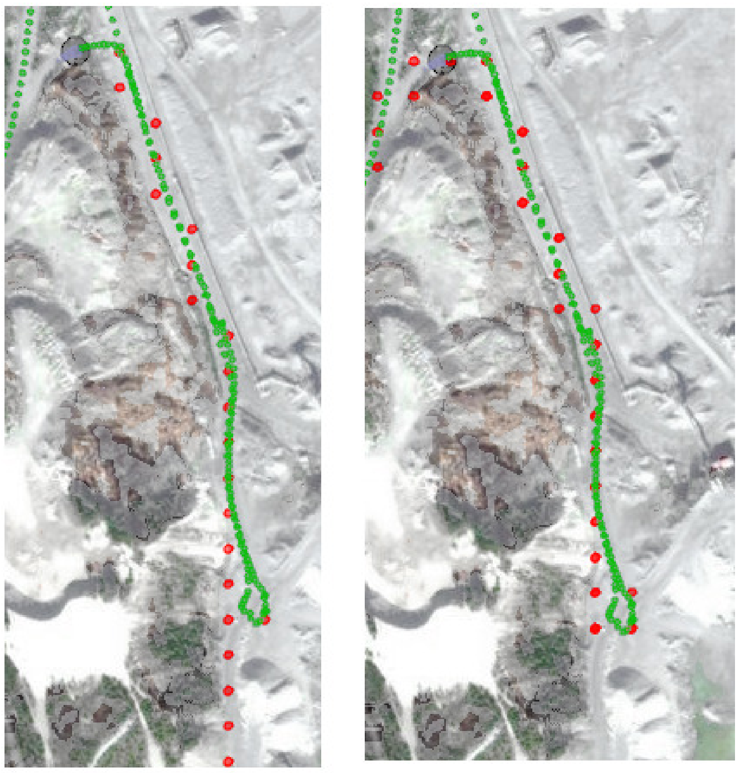

Figure 3.11: Loops disallowed (left) vs allowed (right). Map data: Google, Lantmäteriet/Metria.

the plausibility of loops in the predicted route. In Reference #3 (see Section 4.1.3), when driving in a quarry, loops are comparatively common. Disallowing them ($visit_{lim} = 1$) might be reasonable for regular roads and highway driving, in particular. The same settings gives unexpected behavior, however, in Reference #3. By increasing the tolerance in this case, loops are again allowed. Figure 3.11 shows the prediction at a certain point with loops disallowed (left) and loops allowed (left) ($visit_{lim} = 3$). The actual route taken involves looping around and returning the same way. With loops disallowed, however, the system selects the next most probably route, which is to keep the current heading (south in the picture).

For the on-road driving in Reference #2, however, allowing loops yields a sub optimal result. To rectify this, a speed dependent setting is introduced such that:

$$visit_{lim} = \begin{cases} \alpha, & speed_{current} > 40kph \\ \beta, & otherwise \end{cases} \tag{3.31}$$

Distance calculation

Since the desired output of the system is the road grade as a function of distance, the length of each point of the route needs to be determined. The result of the prediction is a series of pixels that the HDV is predicted to pass through, but the exact distance at each point is unknown. Using the pixel size would only yield a correct value for straight travel through the pixels (direction perpendicular to one of the pixel sides). Therefore, some approximation is needed.

The desired result is an approximation of the travel distance for each and every pixel in the horizon. To approximate the distance that the HDV is assumed to travel to reach a given point, a way of converting WGS84 coordinates is a prerequisite. A method of determining a plausible fine-grained path between the pixels of the horizon can be accomplished in a few different ways:

- Linear travel through each pixel by interpolating linearly between the entry and exit point for each pixel. This is described by Pivén and Ekstrand [16].
- Linear approximation by calculating the distance between two pixels of some distance in the horizon, and division by the same number of data points
- Polynomial fitting to select pixels
- Spline fitting to the entire horizon

Linear interpolation

One of the most straight-forward approaches to calculating the length of the distance is to linearly interpolate between two points. This is done by selecting two close pixels in the horizon with some distance between them and calculating the linear distance between them, as described previously. The pixel coordinates are used, which represents an aliased version of the assumed route. The distance between the center point of two subsequent pixels will not be a very accurate estimation of the actual distance traveled, but by taking two pixels of some distance along the horizon, the aliasing error is diminished.

This distance is then divided by the number of data points between the two pixels to obtain an average “distance per data point” value that is applied to the latest data point. This value can then be re-calculated for each point by using a queue that keeps track of the last few points of the horizon, as it is being constructed.

This approach will give a good estimate for straight road segments, but introduce some error in road segments with curvature.

Polynomial interpolation

Another possible approach to calculating the distance is to use a polynomial interpolation between some selected points, and then calculating the arc length of the polynomial, giving the distance estimation.

Monotonic growth of the x axis is ensured by adding a small value to subsequent points if they are equal.

A problem with polynomial fitting is that for cases of straight travel, the resulting polynomial is a very poor estimation of the route traveled. Figure 3.12 shows an example of such a situation. Three points are plotted to the left, with piecewise linear interpolation shown, and to the right is the same plot with a second degree polynomial fit. Note the difference in axis scale.

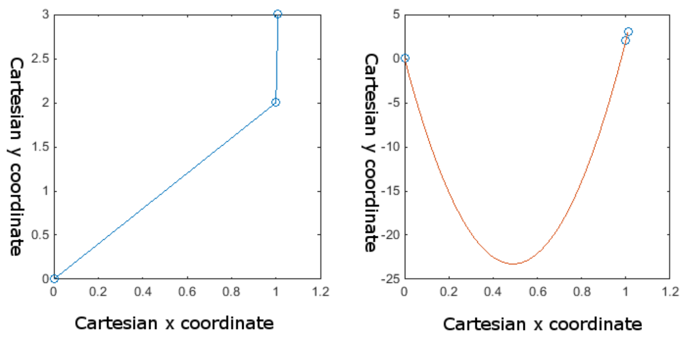

Figure 3.12: Second degree polynomial interpolation of three points

To try and rectify this, more points from the source data are used for the polynomial fit. A cubic polynomial has three unknowns:

$$p_2(x) = a_2x^2 + a_1x + a_0 \tag{3.32}$$

which means that three points is an exact determination of the corresponding polynomial. This is what causes the unwieldy shape of the curve. By adding more points to the source data the system becomes over-determined and solving using the least squares method (Legendre [12]) yields a polynomial that is a more reasonable assumption of the route taken to pass through the original points specified, as shown in Figure 3.13.

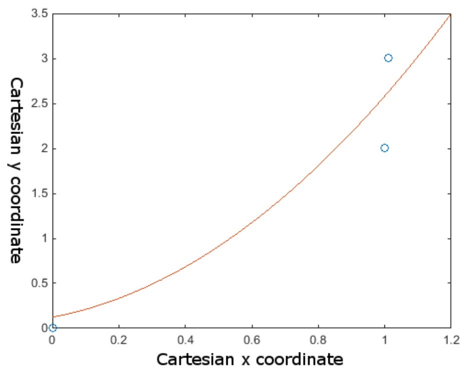

Figure 3.13: Least-squares fit of second degree polynomial to three linearly interpolated points

Applying this to the simulated system gives the result in Figure 3.14, showing a second and third order polynomial interpolation of five points, as well as the linear interpolation.

Note from this figure that the polynomial interpolations are disconnected from the endpoints.

For sharp curvatures, the polynomial that fits within the x-axis that it is being evaluated inside, the length may be significantly shorter than the linear interpolation, causing an underestimation of the distance. A possible solution to this is to interpolate linearly between the endpoints of the polynomial and the start and end pixel.

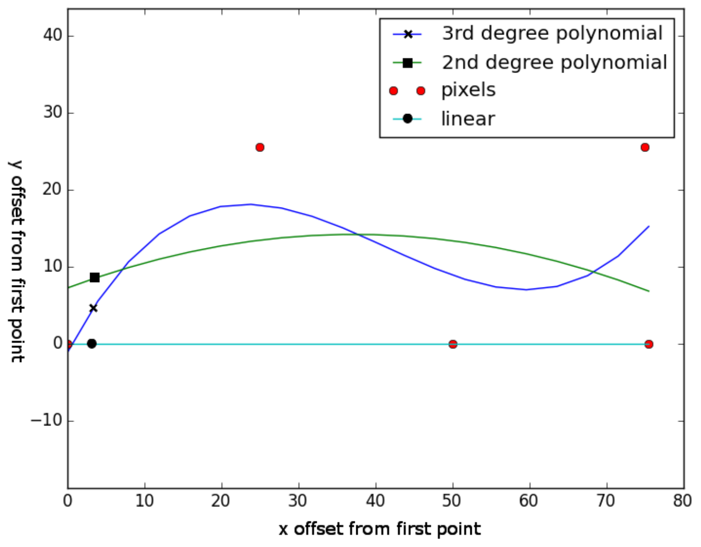

Figure 3.14: Linear, quadratic and cubic least-squares interpolation of points

Splines

Yet another possible approach is to construct a quadratic spline along the points. Since a spline passes through every point specified, the set of pixels is thinned by discarding every *n*th point. Figure 3.15 shows an example of such a spline, with every fifth point used.

The spline differs in previously described approaches in that it is calculated once for the horizon, and the same spline is used to estimate the travel distance at each point.

Heat as a quality measure

Quality implies several properties of a horizon generation system that are of importance.

- Making sure the system does not behave worse than the fallback case
- Minimizing route changes and route planning instability from one prediction to the next
- Determining when to discard the horizon and start anew

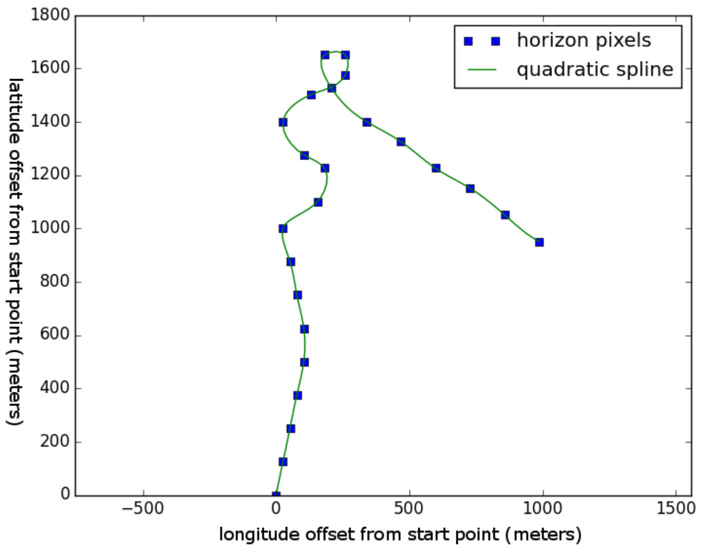

Figure 3.15: Predicted route approximated by using a quadratic spline

On a pixel level

One goal of the robustness is to prevent the incline prediction from deviating significantly from actual road conditions. Returning a positive incline when the actual incline is negative, or vice versa, is considered catastrophic, and in these cases one would like the system to recognize its own uncertainty and fall back to a zero incline prediction.

By keeping track of the number of cold points in the horizon (defined as never having been actually traveled through), and disallowing more than 5 cold points, a fallback is done where the rest of the horizon thereafter is a zero incline slope. This avoids the horizon from deviating from the road, finding another road and returning an incorrect slope prediction that risks being far off the correct value.

One advantage of the heat map based route prediction approach is its inherent ability to quantify the quality of a given horizon. This is done by summing the heat of each pixel that makes up the horizon, producing a total heat value for the entire horizon. If this value is zero, that means none of the pixels have ever been passed through, and the horizon will be equivalent to a fallback with no incline. If the horizon is non-zero, but low, this likely means that the horizon “cuts off” somewhere, and we can resort to a fallback due to not finding a viable path. This may be due to an unexpected path choice, incomplete data or erroneous predicted route. In these cases, this uncertainty may be determined by the horizon heat value. What this means practically is that a conscious choice regarding when to resort to a fallback can be taken based on this value.

To exploit the heat value as a quality measure in a meaningful way, several viable horizons can be constructed to evaluate them on a few different metrics.

Defining the pixel certainty as:

$$certainty_{pixel} = \frac{\left|heat_{highest} - heat_{next\_highest}\right|}{heat_{highest}} \tag{3.33}$$

$$0 \leq certainty_{pixel} \leq 1 \tag{3.34}$$

produces a value at each point in the horizon measuring the certainty of the path choice at that particular point. Equation 3.33 ⇒ Equation 3.34. A value of 0 means that the second highest path, defined as a branch at this pixel, is just as likely as the one chosen, and a value of 1 means that the chosen path is the only one that contains any data whatsoever.

When the certainty dips below a certain threshold, we consider the alternate path by taking the next most probably branch and recursively calculating the horizon for this choice. Using this method, several horizons of high likelihood are derived. They are compared to each other based on difference in road grade and total heat.

The difference in road grade matters because we are keen on avoiding predicting a positive incline when the actual slope in negative, and vice versa, especially for large value predictions. By avoiding making a prediction in cases when alternate routes differ greatly in their predicted slope, the informed choice to fall back to a slope of 0° can be made. By doing so, the system will perform as if no prediction was made, rather than risk performing worse than no prediction.

On a horizon level

Something can be done to improve the system-wide robustness, meaning the series of horizons being produced and finally transmitted. By using the heat values as a basis, we can measure the quality of a given horizon and make sure we always generate a plausible route.

The total horizon heat is used for determining the quality of each horizon. If the heat of a horizon is substantially lower than another one, this likely means that the lower heat horizon either cuts off somewhere, or simply is less traveled. When the heat difference reaches a certain threshold, the choice can be made to disregard the lower heat horizon in favor of a higher heat one. The results of this are explored in Section 4.5.

In order to avoid cold horizons, several horizons of descending likelihood are produced and weighed according to:

$$weight_{horizon} = \frac{heat_{horizon}}{i\,\alpha + 1} \tag{3.35}$$

where i is the horizon number (0 being the first and most likely candidate) and α is a constant. The horizon heat is defined as the sum of the heat of the pixels comprising the horizon.

$$heat_{horizon} = \sum heat_{pixel} \tag{3.36}$$

The other horizons are then found by finding ambiguous points and branching off at these points. The horizon of the highest weight, $weight_{horizon}$, is chosen.

Another possible strategy at this point is to revert to a fallback of zero incline. This is especially useful if one of the horizons predicts a steep incline while the other predicts a steep decline, as this suggests the risk for error is high.

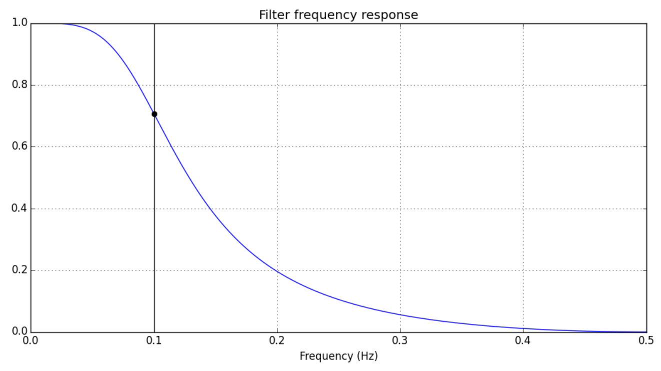

Figure 3.16: Frequency response of a second order low pass filter with a cut-off frequency of 0.2 Hz

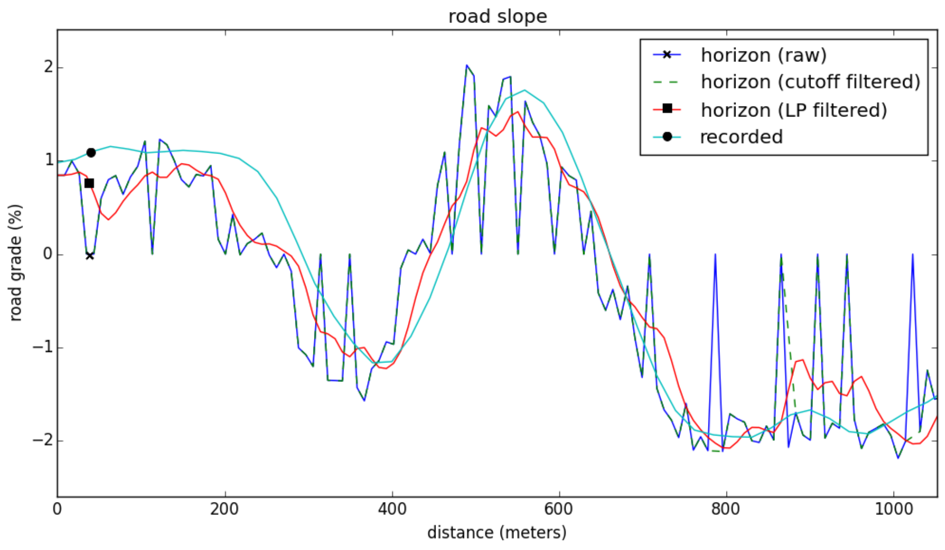

Figure 3.17: Effects of the filters on a route prediction signal

Filtering

Signal noise and measurement uncertainty inherent due to the method of approximating the road slope (as described by Sahlholm [18]) cause the need for output signal filtering. The first step of this filter is a simple cutoff filter for rogue values since at some single points erroneous data is presented either due to measurement noise or transitioning through pixels with missing data. These are removed by considering three points at a time. The difference between the first and second points are calculated and if this values exceeds a threshold, the second point is replaced by a linear interpolation between the first and third points.

The data is then fed through a low-pass filter to smooth it. A second order filter is chosen to minimize phase shift. Figure 3.16 shows a low-pass filter with a cut-off frequency of 0.2 Hz.

This effects of the two filters applied are shown in Figure 3.17.

Horizon transmission

Since the ECU that generates the horizon is not the ECU where the horizon will be utilized for gear selection and cruise control, it needs to be transmitted across a CAN bus with limited capacity. With this in mind, methods for limiting data transmission while simultaneously increasing robustness are developed.

A horizon that is robust enough that it does not need to be recalculated from scratch at every point is desirable. To test this, a horizon $h(x)$, defined as a function of a distance, with the function value representing road grade, can be generated at some point x_0 along a route. For a new horizon $h_{new}(x)$, generated further along the route x_1, the following should hold:

$$h(x) \approx h_{new}(x)\, \forall x \in [x_0, x_1] \tag{3.37}$$

for some tolerance. The benefit of fulfilling this condition is that the horizon can hold for several points, and does neither need to be recalculated nor resent across the distributed network for every new GPS sample. This concerns the reliability of the horizon as a predicted route.

As a first step towards achieving this, the new and old horizons need to be aligned. This is done by excising a number of data points at the start of the previous horizons, since they are now presumably behind the vehicle, giving the new start index $i_{previous}$ as the point with the smallest distance between the two horizons:

$$i_{previous} = i \mid min\left(\left|horizon_{new}(0) - horizon_{previous}(i)\right|\right) \tag{3.38}$$

By examining the first few GPS coordinates, the start offset can be found quickly. If it is not, this means the horizons are too far apart and the previous horizon should be discarded anyway. Although it depends on the horizon spacing, in reality usually only the first two or so points need to be examined. Figure 3.18 shows three non-aligned subsequent horizons, overlaid on top of each other, without alignment. From this figure is visible that they differ only by an offset. Remove the offset by aligning them and they differ only by their end points.

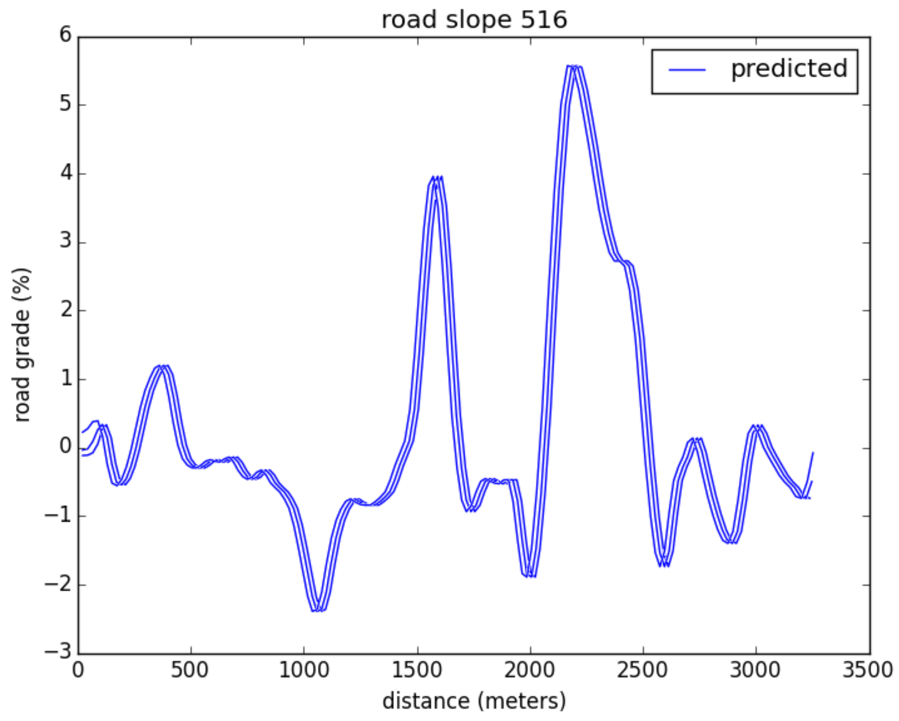

Figure 3.18: Three subsequent horizons, overlaid on top of each other

The desired end result, however, is not actually a prediction of the route; this is merely a means to and end. A road slope function is the final output from the system. Therefore, the other aspect of the horizon quality is to examine the predicted/recorded road slope.

As mentioned in Section 1.2, data transmission capability is severely limited. The ideal case would be building a perfect horizon and incrementally updating the tail of the horizon with new data while removing old data at the head.

The solution for transmission is to replace all data points in the old horizon when $\Delta_i > tol$ with the corresponding data value of the new horizon. This way, only some select data points are re-sent, along with some meta data to place them in the correct order in the horizon, which is to be performed by the target ECU system. A suggested form of meta data for accomplishing this is the distance from the current position, which makes it trivial to find the correct data point to replace by comparing the values. By doing this, points can be sent in any order. This is done in the prototype to assemble the final horizon and measure its error.

The individual point resend strategy means that the distance needs to be recalculated inside the receiving ECU, since the entire horizon is not retransmitted. The proposed solution for this is to use a counter that starts out at zero, and increments by the difference between the distance from the current data point to the previous one at each point. To support this, the difference in position between the current point and the previous one is transmitted, rather than the absolute value. Algorithm 3.5 shows the implementation in the simulation environment.

Retransmission of single points, however, is not supported by the current ADAS Interface Specification ([4]) and implementing this would thus require a custom interface.

Algorithm 3.5 Recalculating point distances in modified horizon

```
if i > 0:
    x_current += aligned_x[i] - aligned_x[i-1]
x_list.append(x_current)
```

Because of this, an alternative approach of resending the entire horizon when any points differs is explored, which is supported in the current production system.

Since bandwidth is severely limited, it may be the case that not every point in the horizon can be sent in its 1 second sample interval. To handle this situation, the new horizon (where the mix of new and old horizon points are determined) is constructed and sent incrementally. A maximum allowed number of points to be resent is implement to limit and control bandwidth in edge cases. By adopting this strategy, the most important (closest to the HDV) points are kept up-to-date and a complete horizon is always guaranteed at the receiving ECU.

Data structures

The chosen data structure governs the memory usage of the map, and it is thus desirable to make it as compact as possible. To store a single pixel in the map, the following generic data structure is used:

```
typedef struct{
        uint32_t x;
        uint32_t y;
        uint16_t slope[N_DIRECTIONS];
        uint8_t heat[N_DIRECTIONS];
} pixel_t;
```

Note that the slope value accuracy has been increased compared to the previous implementation (see Figure 2.5), because 8 bits are not enough to save the values with a satisfying granularity. The x and y coordinates, when using a quadtree, need to be remembered inside the data structure.

Using the optimized algorithm using three heat maps with five bit heat values (see Section 4.2.7) gives a possible data structure as such:

```
typedef struct{
        uint32_t x;
        uint32_t y;
        uint16_t slope[3];
        uint16_t heat; %contains 3 heat values, bounded by
           32
} pixel_t;
```

for a total data storage requirement of 128 bits, or 16 bytes. This data structure is aligned on the 32 bit processor subject to host the implementation. For the planar based road slope format, the slope data is replaced with two scalar values, giving it a lower storage requirement but a larger computational overhead.

Algorithm 3.6 Finding a pixel in the quadtree

```
def pixel_at(self, (x, y)):
    x = int(x)
    y = int(y)
    global pixeltree
    pixel = pixeltree.intersect(bbox=[x-1, y-1, x+1, y+1])
    for candidate in pixel:
        return candidate    #there can be only one
    pixel = Pixel((x, y))
    pixeltree.insert(pixel,
                     bbox=[x-0.1, y-0.1, x+0.1, y+0.1])
    return pixel
```

The heat values are then accessed as follows. By doing this, the heat values can be stored in a compact manner and accessed using bitwise AND operations and bit shifts:

$$heat_1 = (0000000000011111 \wedge heat) \tag{3.39}$$

$$heat_2 = (0000001111100000 \wedge heat) \gg 5 \tag{3.40}$$

$$heat_3 = (0111110000000000 \wedge heat) \gg 10 \tag{3.41}$$

Using a quadtree

To quickly find and address a desired pixel, a quadtree is utilized, as described in the Background chapter. A quadtree is normally used for finding points on a continuous range (such as WGS84 coordinates). Since discrete Cartesian coordinates are used in the implementation, each pixel is given an arbitrary size that is sure to fit within its actual, discrete, dimensions. Algorithm 3.6 shows how storing and recalling pixels using a quadtree is implemented.

Chapter 4
Results

In this chapter, results of different approaches and parameter settings are presented. The first section explains the methodology with which the system is evaluated. The next section is concerned with finding the optimal (highest performance yielding) parameters for the heat map based system. Then follows sections with results of managing the horizon transmission strategy, horizon weighing using heat values and decoupled road grade storage. The last section contains an estimation of the storage requirements for the map.

Evaluation methodology

One of the core parts of this thesis has been to come up with a reliable evaluation methodology in order to, as objectively as possible, compare the performance of different approaches. This section presents the reader with an explanation of how this was accomplished.

Performance assessment

The main basis on which system performance is measured is the average error for several reference routes. A number of CAN logs (traces) collected from actual HDVs are played back to the system, each comprising travel along a certain route. By doing this, driving along these routes the same number of times as the number of traces is simulated, creating the map as it would exist in the vehicle at this point.

After building the map, another, previously unused, CAN log (trace) is then used to simulate novel driving along a similar, but not identical, route. At equally (temporally) spaced points along this trace, a horizon of a static length is generated and compared to continuation of the actual log, and the error between the predicted road grade and the recorded road grade of the trace is compared at each point. Finally, the average error is calculated.

$$err_{avg} = \frac{\sum_{i=0}^{n} |slope_{horizon}(i) - slope_{recorded}(i)|}{n}, \; dist(n) = 2500 \qquad (4.1)$$

As mentioned earlier, a horizon length of 2,500 meters is sufficient.

Visualization

A visual approach is used to display system characteristics. By doing so, route prediction choices can been easily seen.

This chapter contains several visualized road segments and predictions. Figure 4.1 shows an example of such a visualization. It consists of a data overlay on a map. The data is visualized as differently colored dots depending on what they represent.

- The large semi-transparent gray dot represents the current position of the HDV at the current data point.
- Blue dots (behind the HDV dot) in decreasing size show the previous GPS locations of the HDV.
- Red dots (slightly transparent) comprise the horizon as predicted from the current position. Points that are passed through more than once are opaque.
- Green dots (smaller than the red dots) are the actual positions that the HDV passed through after proceeding from the current data point. In the ideal case, the red dots should follow the path of the green ones.

Accuracy is measured by calculating the predicted slope function from the horizon and comparing to the actual recorded slope when continuing (green dots). For data sets, the error for each horizon is averaged.

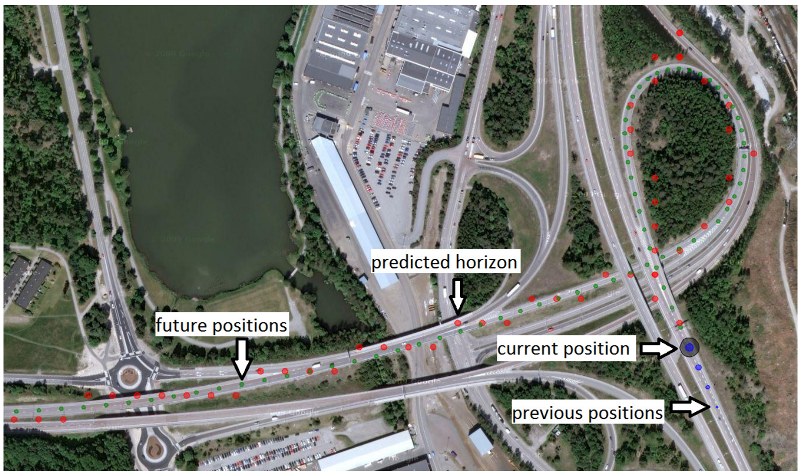

Figure 4.1: Visualization of a road segment. Map data: Google, Lantmäteriet/Metria.

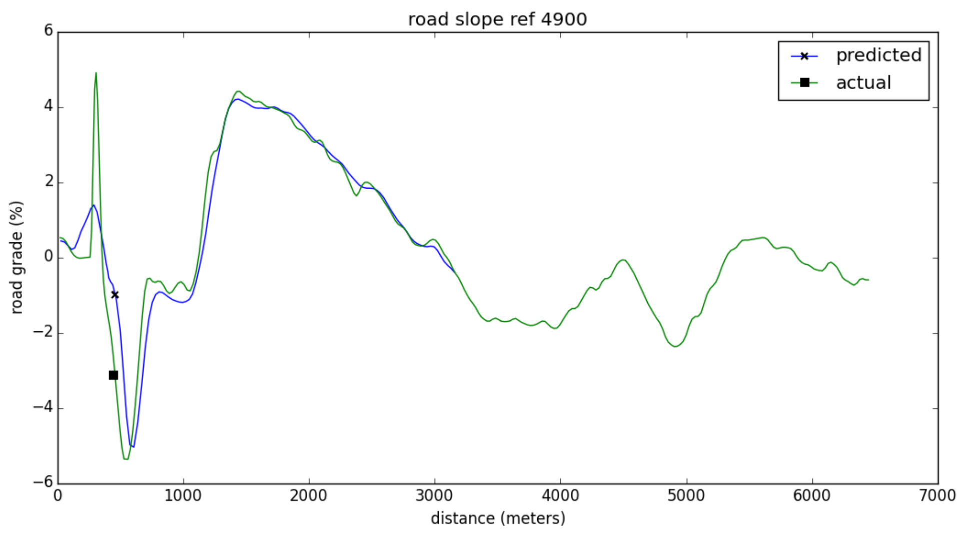

Figure 4.2: Slope plot for the corresponding segment

Figure 4.2 shows the corresponding slope plot for the segment. In this plot, the predicted road grade, produced from the horizon, is plotted in a blue color. The actual slope recorded after proceeding in plotted in green. The average error is computed up to a desired horizon length as the absolute difference between the two plots. Choosing 2,500 meters yields an average (per point) error of 0.182 percentage points for this particular segment.

Reference routes

In order to measure system performance, a few references are defined which are used to compare different algorithms and gather experimental data against a common baseline.

Reference #1: 10 manually selected segments along a route, containing road crossings, acceleration ramps and roundabouts. These points are especially challenging for route planning.

Reference #2: Data consisting of 250 minutes of driving, with the predicted horizon sampled every sixtieth second. The route taken starts in Södertälje and follows route 4 past Nyköping, makes a turn before Norrköping and passes Katrineholm and Mariefred on the way back to Södertälje. This route represents typical long haulage driving. Figure 4.3 shows the data.

Reference #3: Data from driving in a quarry. This data set is challenging both because routes contain many similar possible routes, as well as tight turns, and inclination differs greatly, increasing the cost of incorrect prediction. It is also highly relevant, since it represents a situation where commercial road and slope data is typically unavailable. The reference covers 150 points, separated temporally by 60 seconds. Figure 4.4 shows the data.

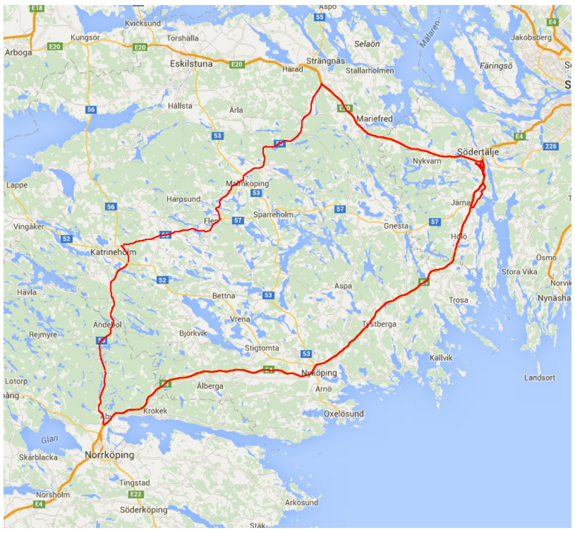

Figure 4.3: Reference #2. Map data: Google.

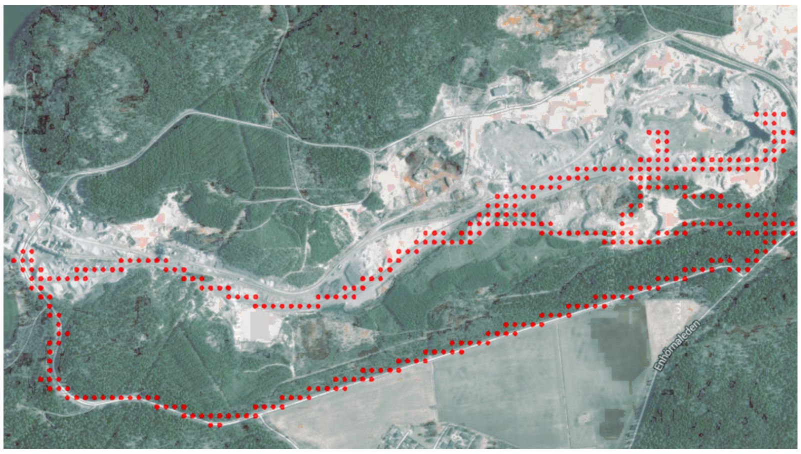

Figure 4.4: Reference #3. Map data: Google, Lantmäteriet/Metria.

Design choices and parameters

In this section, approaches and parameters for the heat map based system are examined individually, to obtain comparative results. Unless otherwise stated, Reference #2, as described in the previous section, is used for calculating error figures, and the number of historical traces is 10.

The baseline for the errors is the case where no prediction is used, which is analogous to assuming a constant slope of 0°. This gives an average error of 1.28, which is defined as 100% error. Errors presented in this chapter are expressed as fractions of this value. Table 4.1 shows the baseline error figures for each of the reference routes. Note that this value is the average absolute road slope along the route (i.e. the average deviation from 0).

route	avg road slope
Reference #1	1.63 ≡ 100%
Reference #2	1.28 ≡ 100%
Reference #3	4.43≡ 100%

Table 4.1: Baseline values (errors when predicting a constant 0 degree slope)

Pixel size (side, meters)	average error
10	11% (0.145)
15	10% (0.128)
20	9.7% (0.124)
25	13% (0.163)
30	14% (0.181)
35	17% (0.212)

Table 4.2: Error as a function of pixel size

Pixel size

The size of the pixels in the raster map has a great effect on several parameters of performance, and is also dependent on other parameters and the approach which is used for the prediction.

Overall, a balance between several different factors needs to be considered for a given pixel size to work well.

Table 4.2 shows the effect of increasing pixel size on the predicted route accuracy in the directional algorithm.

Distance calculation

The results of the chosen distance calculation approach is shown in Table 4.3. For all approaches, five points are interpolated between. The least squares fit method is used to find the polynomials. For the natural version, with no fixed endpoints, the 3rd degree polynomial performs somewhat better because of its ability to get closer to the endpoints. For the version with linear interpolation between the endpoints of the polynomial, and the start and end pixels, however, the second degree polynomial generally gives rise to more natural-looking estimated curvatures, as evident if several interpolations are plotted and compared to each other.

The approaches without fixed endpoints cause the polynomial to be significantly shorter than the actual traveled distance for some curvatures. This effect is clearly visible when plotting the slope horizon as in Figure 4.5. See also the visualizations in Section 4.7.

approach	avg error
linear interpolation	9.7% (0.124)
2nd degree polynomial interpolation	41% (0.519)
3rd degree polynomial interpolation	24% (0.312)
2nd deg poly with linear endpoints	10% (0.133)
3rd deg poly with linear endpoints	11% (0.135)
quadratic spline	17% (0.212)

Table 4.3: Distance calculation approaches

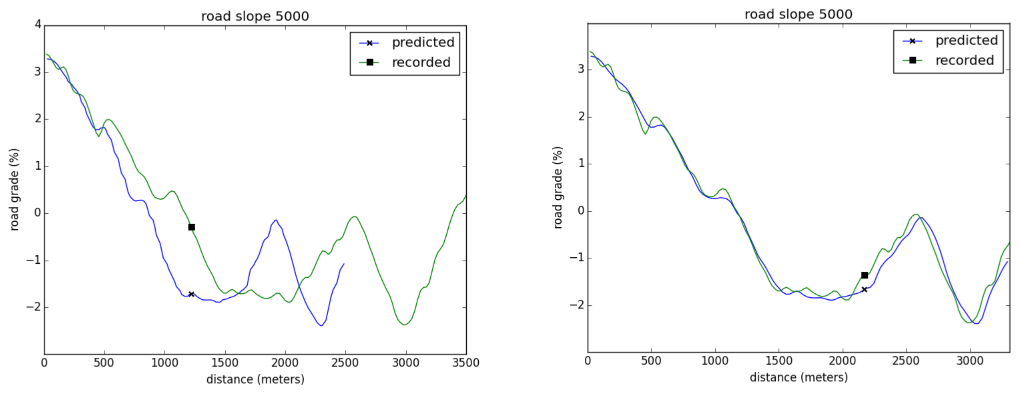

Figure 4.5: Second degree polynomial distance estimation: natural (left), with linear endpoints (right)

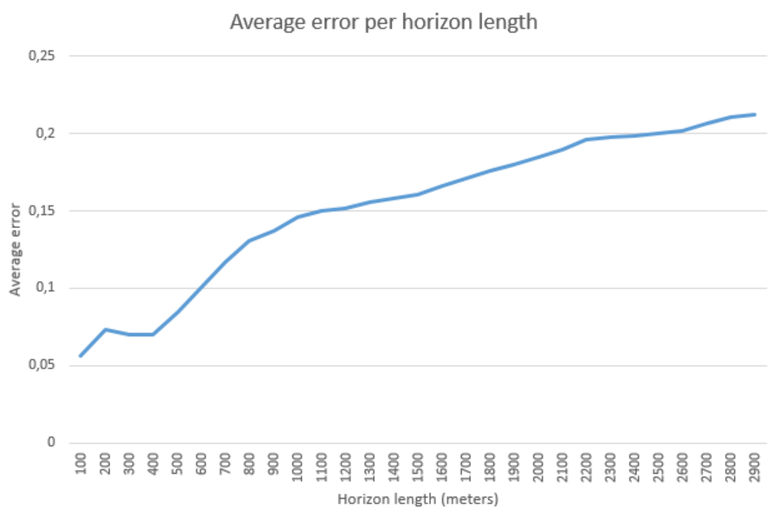

Figure 4.6: Error as a function of horizon length

Horizon length

The longer the predicted horizon, the higher the error will be. The reason for this is twofold:

1. Between each point pair in the horizon, a distance estimation has been made. This estimate will grow less and less accurate the further removed from the start position of the horizon because some error is introduced at each point, depending on the accuracy of the distance estimation method.

2. The number of route choices increases with travel length, meaning that our route is less certain the farther the travel.

Plotting the error as a function of the horizon length gives us Figure 4.6. To gather the data for this chart, average errors are computed for separate runs with different horizon lengths.

To show a more meaningful correlation, the average error is again calculated, but each horizon is cut in 100 meter long pieces. The average error is calculated for each such piece (sliding window). The results of this are visualized in Figure 4.7. The result seems to be a linear correlation between the distance between the piece and the horizon start, which seems reasonable (see also the linear trend line). Worth noting, however, is that the derivative is not very steep, meaning that long horizon may be used without introducing a dramatical amount of error.

The data is also more valuable the more immediately useful it is, meaning the start of the horizon and its higher quality data carries more value than the data later on. This is because the most immediate prediction determines when an incline or slope will begin or end, making the timing important. But the more remote the data, the less important the exact timing of it. The knowledge of whether there will be an incline or slope and its approximate location is important, but the exact timing or height of the gradient is of lesser importance.

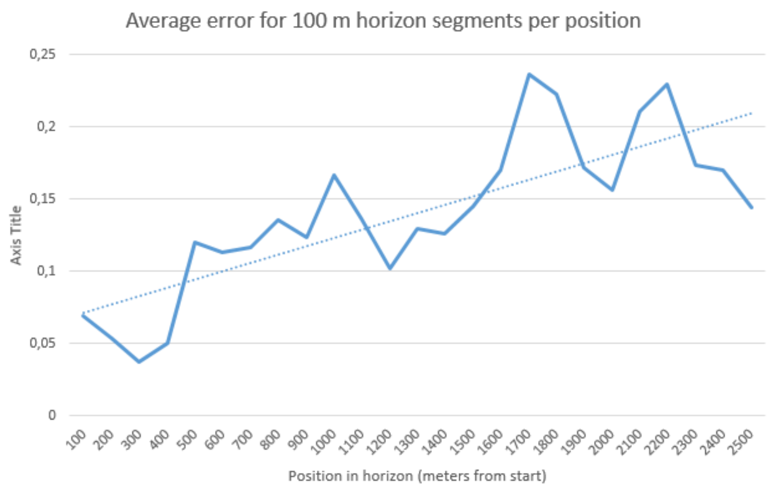

Figure 4.7: Error for 100 meter sliding window segments of the horizon, at different positions in the horizon

# directional heat maps	average error
1	11% (0.140)
2	14% (0.180)
3	12% (0.152)
4	14% (0.178)
10	20% (0.256)

Table 4.4: Error as a function of heat map directions, for 5 traces

Heat map directions

For Reference #2 used as a basis for the data in Table 4.4, a single heat map gives the best result. This is interesting, as it would require less overhead. But when delving further into this anomaly, it becomes apparent that the increased accuracy in the single heat map case stems from the fact that the five traces the map is based on all combine into more data for the single heat map, rather than being spread out over several heat maps. Running the simulation again, this time with ten traces, indicates that this is the case. Results are shown in Table 4.5.

A single heat map is only effective when travel normally occurs only in one direction

# directional heat maps	average error
1	15% (0.198)
2	12% (0.159)
3	9.7% (0.124)
4	12% (0.153)
10	20% (0.255)

Table 4.5: Error as a function of heat map directions, for 10 traces

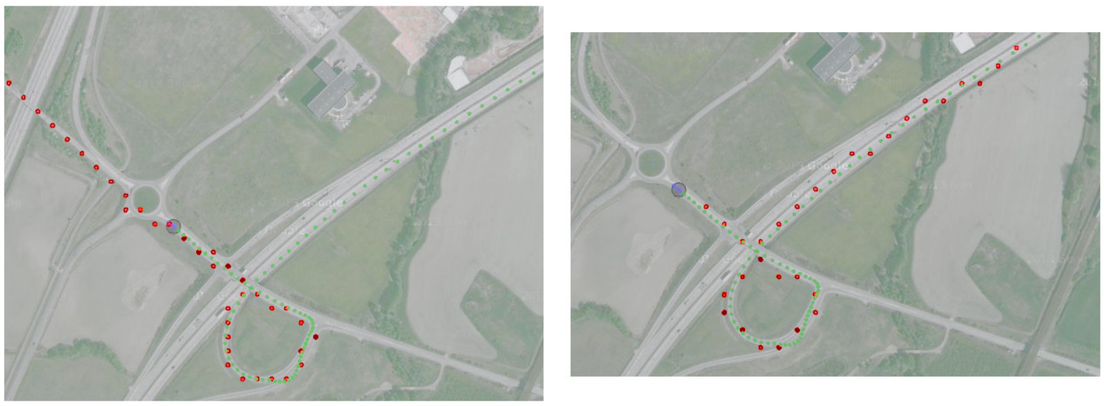

Figure 4.8: Acceleration ramp, with single heat map (left) and four directional heat maps (right). Map data: Google, Lantmäteriet/Metria.

# directional heat maps	Reference #1	Reference #2	Reference #3
1	47% (0.773)	15% (0.198)	97% (4.28)
3	26% (0.430)	9.7% (0.124)	48% (2.11)
4	46% (0.752)	12% (0.153)	50% (2.22)

Table 4.6: Average error as a function of heat map directions, summary

in each pixel. In the recorded data set in Reference #2, travel is only performed in one direction at any given highway segment. However, when examining some more challenging road situations, it becomes apparent that using a single heat map with any reasonable pixel size means the predicted route tends to drift between opposing lanes.

This phenomenon is eliminated by increasing the number of heat maps, which means that, for example, an eastbound lane will not ever be selected when traveling west. See Figure 4.8 for a visualization of what happens when only using a single heat map for road situations other than straight highway travel, as opposed to four. In the single heat map case, the predicted horizon follows the acceleration ramp to the highway but decides to take an abrupt turn and return the same way it arrived, whereas with four directional heat maps, the highway is entered correctly.

The results are confirmed for the other References in Table 4.6. Note that too many directional heat maps invoke a sparseness that degrades performance, which is further discussed in Section 5.1.3.

Road grade format

Two options for storing the road grade have been implemented; storing the slope as discrete values, one per each heat map direction, or storing the road grade as a plane within each pixel. The idea is that the plane will always guarantee consistent data, and might produce a better grade prediction because it allows for entering pixels in any direction. This assumes

road grade format	avg error
Discrete (3 directions)	9.7% (0.124)
Planar	15% (0.192)

Table 4.7: Average error as a function of heat map directions, summary

setting	avg error Ref #3	avg error Ref #2
$visit_{lim} = 1$	64% (2.84)	18% (0.236)
$visit_{lim} = 3$	48% (2.11)	12% (0.150)
$visit_{lim} = \begin{cases} 1, & speed_{current} > 40kph \\ 3, & otherwise \end{cases}$	48% (2.13)	18% (0.233)
$visit_{lim} = \begin{cases} 2, & speed_{current} > 40kph \\ 3, & otherwise \end{cases}$	48% (2.11)	9.7% (0.124)

Table 4.8: Error for different configurations of allowing or disallowing loops

a plane in a small enough pixel approximates the actual road topography well enough. Table 4.7 shows the performance of using the planar road grade format as compared to a discrete approach. Three directions are chosen because this gives the lowest error, as explored in the previous section.

Loops and off-road conditions

To evaluate the system performance in off-road conditions, traces from driving in a quarry are examined. A major source of error in this case turns out to be the limited amount of permitted visits to a pixel in a single horizon, intended to eliminate loops.

By testing, the solution to allow different numbers of visits depending on travel speed is shown to produce the best results in both highway and quarry situations; allowed loops in the quarry and disallowed loops at highway driving, see Table 4.8.

Overall system performance in Reference #3 is shown in Table 4.9. The average errors are, in general, larger for Reference #3 than the previously examined cases, the reason for which being the steep slopes present in the quarry. There are inclines as steep as 15º. Horizon length is 500 meters.

The figure obtained in this table might seem excessively high, especially compared to previous results. But consider the horizon plot in Figure 4.9. It is evident from this figure that the high derivative of the (noisy) road grade is such a situation causes the error figure to grow large, which the predicted horizon still follows the actual slope.

Aging

The heat map based road map needs some sort of aging to avoid the heat values of each pixel from exceeding the maximum possible value of the selected data type.

algorithm	avg error	rel error
no prediction	4.43	100% (baseline)
directional algorithm	3.42	77%
heat map algorithm	2.11	48%

Table 4.9: System performance when driving in the quarry

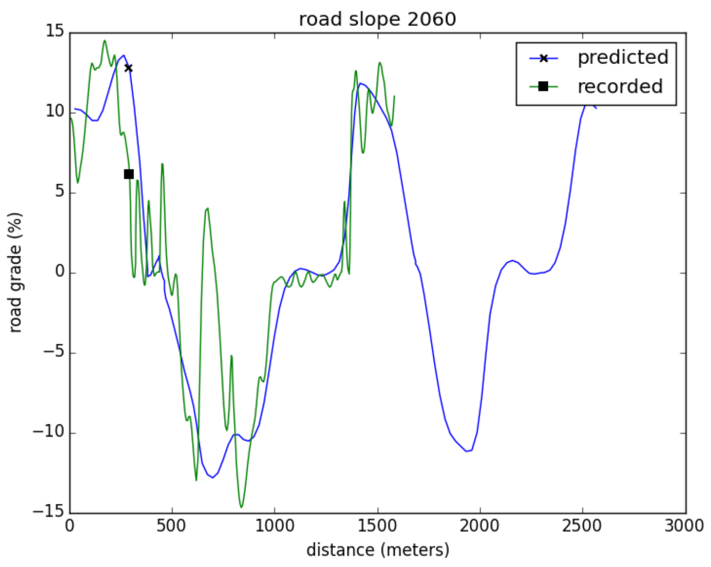

Figure 4.9: Horizon plot for a segment in the quarry

approach	30 traces	300 traces
no aging	13% (0.167)	14% (0.179)
-1 when >16	11% (0.140)	12% (0.159)
-1 when >32	10% (0.128)	12% (0.151)
-1 when >64	13% (0.168)	12% (0.158)
*.95 when >16	11% (0.140)	15% (0.192)
*.95 when >32	10% (0.128)	12% (0.155)
*.95 when >64	13% (0.168)	12% (0.150)

Table 4.10: Effects of aging on accuracy

# previous traces	avg error (directional)	avg error (heat maps)
0 (no prediction)	100% (1.28)	100% (1.28)
1	73% (0.934)	13% (0.164)
5	53% (0.677)	12% (0.152)
10	47% (0.604)	9.7% (0.124)

Table 4.11: Average error for the grade prediction of many road segments (Reference #2) for horizon length of 2500 meters

Both simple subtraction and multiplying with a scalar smaller than one when one of the heat values has reached a certain value, affects prediction accuracy. The chosen weighing parameters for calculating the heat are tested on lower trace maps, and are therefore biased in favor of values typically found in such maps. Therefore, the prediction actually performs slightly worse as the number of GPS traces increases. Aging proves a useful tool in rectifying this problem. See Table 4.10 for a comparison. For the 300 trace run, the first 30 traces were repeated 10 times.

The maximum value of 32 gives the best result according to simulations, which would require 5 bits to store ($2^5 = 32$). Since the ideal number of heat maps seems to be 3, this would require a total of 15 bits, meaning all three values could be saved as a single 16 bit integer.

After some experimentation, the best approach seems to be subtracting all values except the current one if the current value is at its maximum, or otherwise increase by one. This is very computationally light as it only requires a handful of add operations.

System performance

Since the value of interest is the road slope, errors are calculated based on this measure. Running the directional algorithm implemented based on Pivén and Ekstrand [16] (second column, “avg error (directional)”) as well as the heat map based algorithm for Reference #2 yields the results in Table 4.11.

One advantage with that might not be obvious at first is the road length calculation in the heat map based algorithm. Whereas the direction based algorithm constructs its path based on where the predicted position happens to end up according to the saved direction

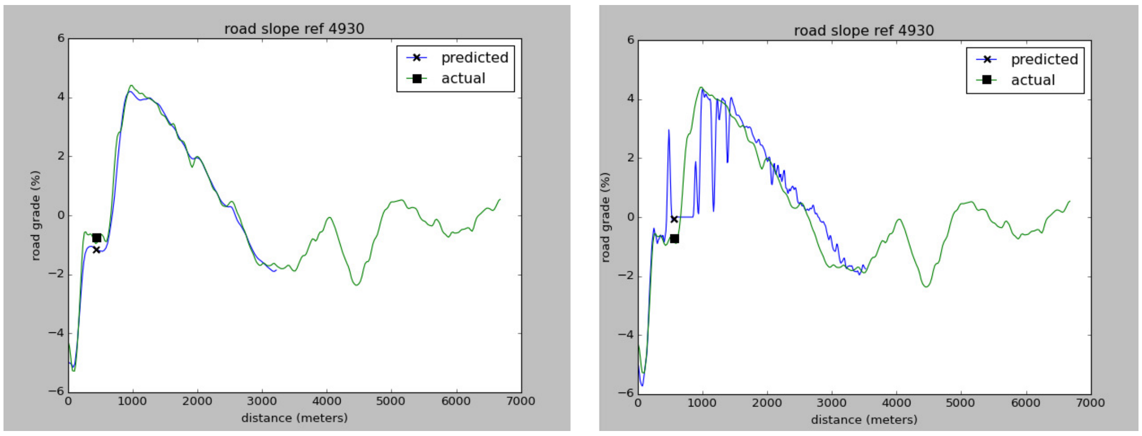

Figure 4.10: Heat map based prediction (left) vs directional prediction (right)

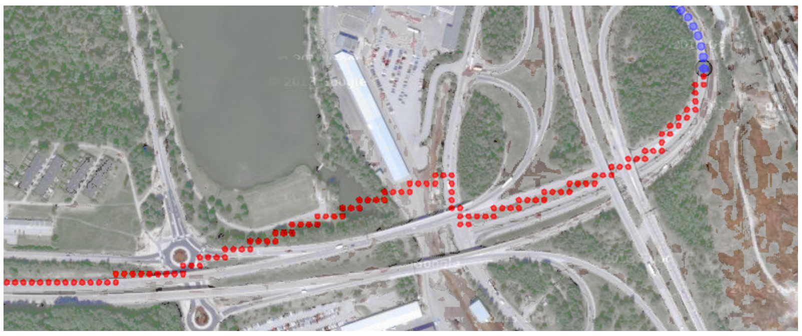

Figure 4.11: Erratic behavior of directional algorithm in a select situation. Map data: Google, Lantmäteriet/Metria.

(which may be skewed; remember than passing through the same pixel at different angles different times will yield a final predicted direction as the average between these two directions, possibly pointing to some undesired middle ground position). This means the path taken might cut corners too tight or too widely. The heat map based approach, on the other hand, since it gives priority to pixels most often traveled through, is more likely to produce a pixel-level accurate prediction. This means that the predicted length of the road is more accurate, yielding a predictive curve that is more closely aligned to the reference curve, thus minimizing the average error.

Figure 4.10 shows the difference in prediction quality between the heat map algorithm and the directional algorithm when driving on a highway above another road segment, and the predicted routes for this graph are shown in Figure 4.11 for the directional algorithm and Figure 4.12 for the heat map based algorithm.

Using a high pixel size introduces another phenomenon, namely subsequent location points falling inside the same pixel, causing the heat counter to be increased multiple times. Through experimental tuning this is found to introduce an error. By checking the pixel against the previous recorded pixel and ignoring subsequent passes through, the system behaves as expected with increasing number of traces (meaning that a higher amount of historical traces does not lead to a decline in prediction accuracy).

Table 4.11 shows the effect of different number of traces on the prediction result and

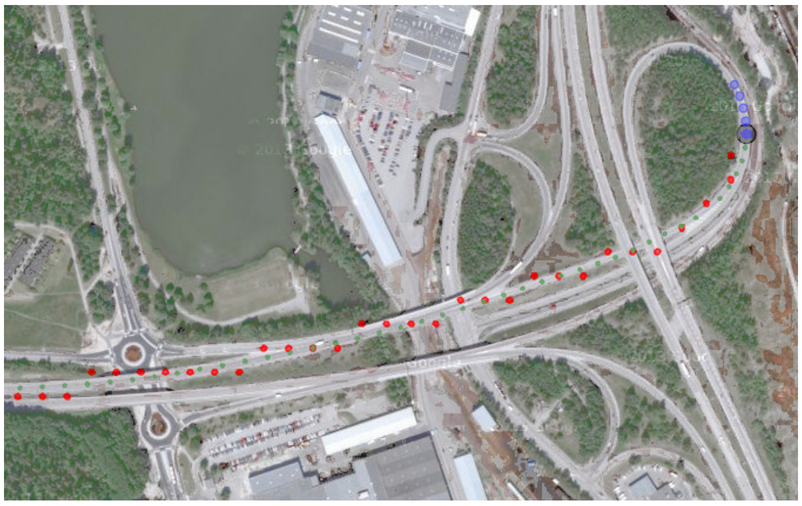

Figure 4.12: Heat map based algorithm in the same situation. Map data: Google, Lantmäteriet/Metria.

route	avg error (directional)	avg error (heat maps)
Reference #1	69% (1.13)	26% (0.430)
Reference #2	13% (0.164)	9.7% (0.124)
Reference #3	77% (3.42)	48% (2.11)

Table 4.12: Average error for the grade prediction of the reference routes, for 10 previous traces

compares system performance between the directional and heat map based prediction algorithms. The more often the vehicle has traveled a certain road, the more accurate future predictions along that road will be. In Table 4.12 is shown an overview of system performance for all three reference routes, using the optimal parameters as determined in the previous section.

Horizon transmission

Since the route prediction is performed in one ECU but the data is utilized in another one, the horizon needs to be transmitted over CAN.

Horizons are produced continually, generating a completely new horizon at each point. It is however, desirable not to send the entire horizon every time because of bandwidth limitations.

If the previous horizon (already sent) is determined to be accurate enough according to some tolerance, new data can be appended to the end of the current horizon. If, on the other hand, the new horizon differs significantly and it is determined that the difference is likely a permanent course change from the route prediction algorithm, the current horizon needs to be discarded and re-sent.

By implementing some strategy to avoid re-sending the horizon at every single point, significant bandwidth is saved. Table 4.13 shows the difference in errors obtained and

strategy	avg err	payload bandwidth	total TX	resent points
(1)	0.119	4.69 kbps	7,617 KiB	100%
(2)	0.167	0.21 kbps	334 KiB	0%
(3), for $\Delta_i > 0.5$	0.125	0.40 kbps	658 KiB	4.4%
(3), for $\Delta_i > 0.1$	0.119	0.43 kbps	704 KiB	5.1%
(3), for $\Delta_i > 0.0$	0.119	0.44 kbps	722 KiB	5.3%
(4), for $\Delta_i > 0.0$	0.119	0.48 kbps	790 KiB	6.3%

Table 4.13: Effects of bandwidth management

the bandwidth by changing the bandwidth management strategy. The route driven is a complete simulation of travel from Södertälje, passing Nyköping and traveling back (see Reference #2). Instead of sampling the horizon at certain interval, the horizon is continually generated once per second (one for every sample point) to simulate the bandwidth effects in a real-world scenario. This means that the values will be slightly different than previous figures.

All simulations are based on a horizon point size of 4 bytes. This fits one 16-bit unsigned integer that represents the distance and one 16-bit fixed point value for the road inclination. This means that two data points fit inside the payload of a single CAN message.

A 1 Hz horizon request rate is assumed.

These strategies are evaluated:

1. Always re-send. This is the naïve solution where a new horizon is generated for every movement in the map, and then sent over the CAN network.

2. Only append new points. The old horizon is always kept and as the vehicle travels further, new data points are simply appended at the end of the horizon, and passed data points are routinely discarded as they are passed.

3. Re-send points with high difference. The new horizon is compared to the previous one and any road slope data points whose difference Δ_i exceed a certain threshold are re-sent individually. This is not supported by the current ADAS Interface Specification ([4]). The distance for each point is recalculated as described in Section 3.8.

4. Re-send entire horizon when a deviating point is found, according to the criterion in (3). This strategy is interesting only because it is supported by the ADAS Interface Specification.

The figures in the table are inconsistent with other measurements on Reference #2, because the error is calculated for every single data point as opposed to points spaced by 60 seconds, in order to produce horizons that can align. This was necessary to collect applicable data.

The columns (from left to right) describe: the strategy used for the test, the absolute average error, the required bandwidth for just the payload portion of the CAN message, the total amount of data transmitted for the complete loop between Södertälje and Norrköping and lastly the fraction of data points that were ever re-sent.

strategy	avg err	payload bandwidth	total TX	resent points
(1)	2.10	4.69 kbps	5,566 KiB	100%
(2)	4.29	0.07 kbps	83 KiB	0%
(3), for $\Delta_i > 0.0$	2.09	0.80 kbps	955 KiB	16%
(4), for $\Delta_i > 0.0$	2.08	1.25 kbps	1,481 KiB	25%

Table 4.14: Effects of bandwidth management on Reference #3

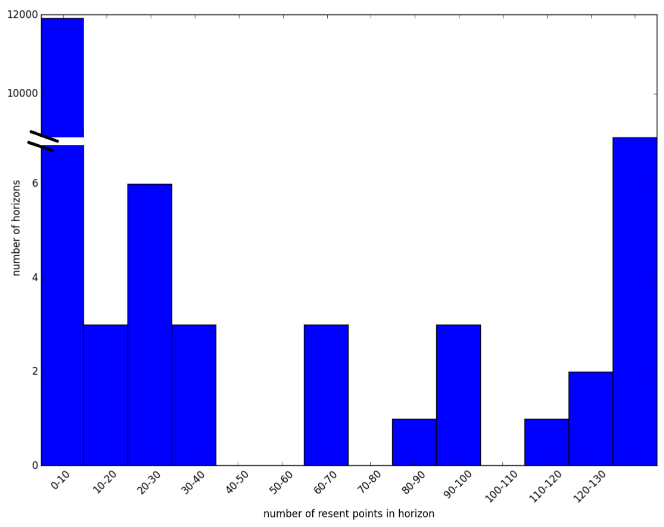

Figure 4.13: Plot showing the number of horizons (y axis) for which a given amount of points (x axis) were resent with strategy (3), for $\Delta_i > 0.0$, for Reference #2. Note the break in the y axis.

Trying out the bandwidth transmission management strategy for Reference #3 results in the figures presented in Table 4.14.

There is, however, a metric that is important to maintaining high system performance when it comes to the transmission strategy. If a 1 Hz horizon generation is used, in the cases where many points along the horizon need to be resent, there may not be enough time to resend all the points within the sample interval. This will lead to performance degradation in the receiving ECU system. To try and measure this, the strategy used for row 5 in Table 4.13 is used. When each horizon is considered, the number of points that had to be resent is recorded. A plot is then made that shows the number of horizons as a function of how many points in that plot had to be resent. The x axis shows the number of points that had to be resent, and the y axis represents for how many horizons this number of points had to be resent. It is thus desirable to have as low span of values as possible. Figure 4.13 shows the resulting plot. For more than 99% of all horizons, not a single point needed to be resent.

Figure 4.14 shows the same data calculated from the Reference #3 data set. This reference route is more densely populated with crossings which gives rise to more uncertainty, as evident by the higher fraction of completely resent horizons. Still, the number of resent

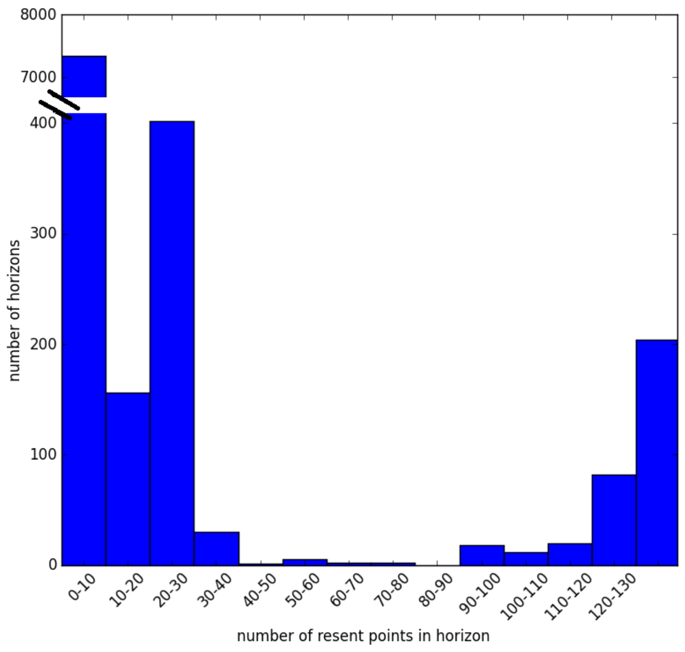

Figure 4.14: Plot showing the number of horizons (y axis) for which a given amount of points (x axis) were resent with strategy (3), for $\Delta_i > 0.0$, for Reference #3. Note the break in the y axis.

points is low.

As seen in Figure 4.14, for the challenging data set in the quarry, all points of the horizon were resent in roughly 200 of the produced horizons. This is a small fraction of the total amount of horizons generated, but is still undesirable. To avoid doing this, the number of allowed changes per horizon can be limited. By doing so, the points closest to the vehicle will be prioritized, as the road grade most immediately ahead of the vehicle has the most bearing on system performance. In the case of a complete route change, this will ensure that the horizon is smoothly replaced over the course of several cycles, each time updating the horizon. Table 4.15 shows the result of applying this strategy in conjunction with transmission strategy (3), for $\Delta_i > 0.0$.

Setting the limit, lim_{resend}, to for example eleven means that, since two points can be sent per CAN message, one new point at the end of horizon plus eleven resent points will result in the transmission of a total of six CAN messages. The maximum desired amount of CAN messages can be controlled by adjusting this parameter. In Figure 4.15 is shown corresponding graphs for the number of horizons as a function of how many points were resent, with different limits. Note that for $lim_{resend} = 11$, the number of horizons in the first and second bar are almost equal. This is because the number of horizons with 0 resent points decreases because refreshed points are instead transmitted more evenly across subsequent horizons.

strategy	avg err	payload bandwidth	total TX	resent points
no lim_{resend}	2.10	0.80 kbps	955 KiB	16%
$lim_{resend} = 6$	2.13	0.28 kbps	329 KiB	4.4%
$lim_{resend} = 11$	2.09	0.33 kbps	397 KiB	5.7%
$lim_{resend} = 31$	2.10	0.47 kbps	562 KiB	8.7%
$lim_{resend} = 51$	2.10	0.57 kbps	672 KiB	11%

Table 4.15: Effects of point resend limit on Reference #3

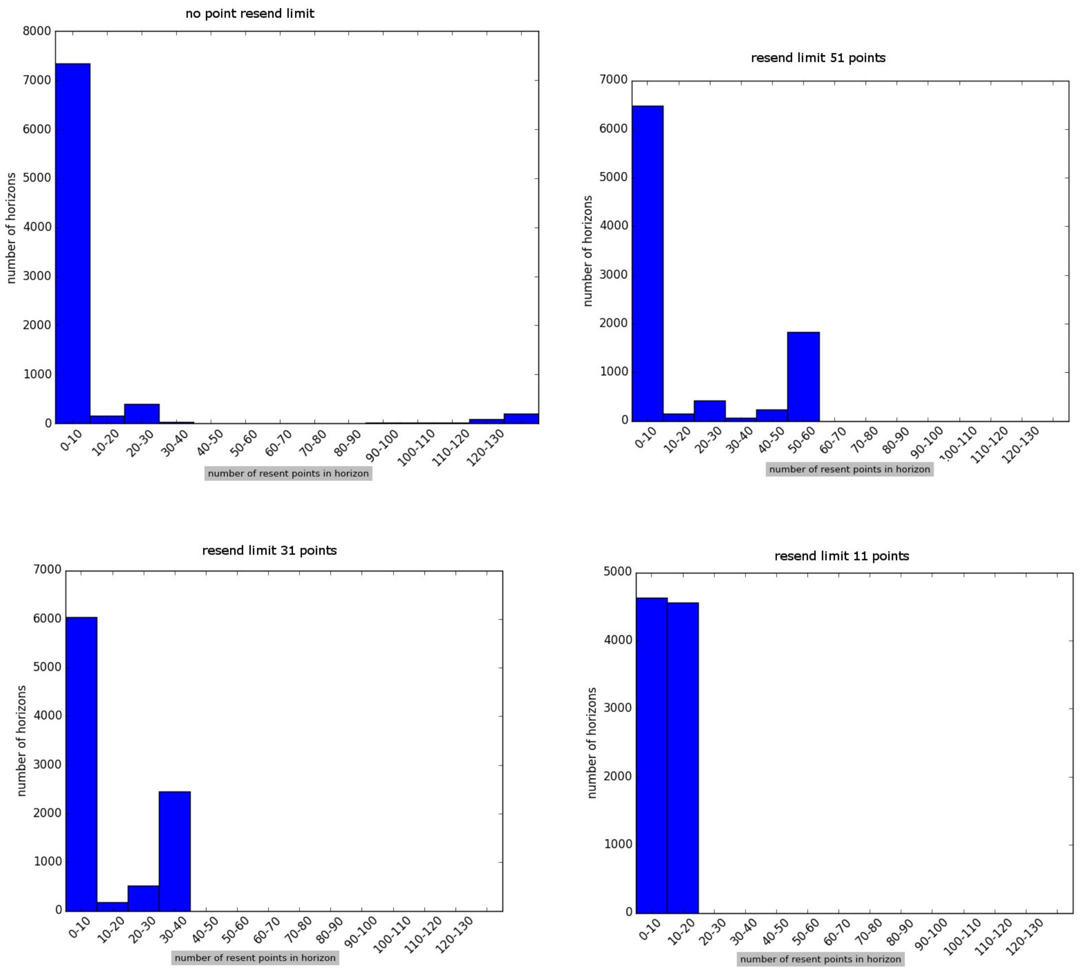

Figure 4.15: Resent points when limiting the maximum allowed points to resend, for Reference #3. From left to right: progressively lower resend limit.

approach	avg error
always use the first horizon	9.7% (0.124)
$\alpha = 0.5$, $certainty_{pixel} < 0.2$, 5 horizons	8.9% (0.114)

Table 4.16: Choosing among several horizon candidates

Heat as a quality measure

As explored in the previous chapter, the heat values of pixels and cumulative heat values for horizons can serve as a sort of quality measure. This section presents the result of applying this to increase horizon quality.

On a pixel level

One goal of the robustness is to prevent the incline prediction from deviating significantly from actual road conditions. Returning a positive incline when the actual incline is negative, or vice versa, is considered catastrophic, and in these cases one would like the system to recognize its own uncertainty and fall back to a zero incline prediction.

By keeping track of the number of cold points in the horizon (defined as never having been actually traveled through, and consequently having heat values of zero), and disallowing more than five cold points, a fallback is done where the rest of the horizon thereafter is a zero incline slope. The idea is to avoid having the horizon deviate from the road, finding another road and returning an incorrect slope prediction that risks being far off the correct value.

This strategy unfortunately also eliminates cases where the prediction loses its way and then finds it again, and will discard such horizons due to their uncertainty. The end result is a 3.9% increase in the average error on Reference #1, and unchanged performance on Reference #2 and #3. Therefore, this idea was not investigated further.

On a horizon level

To find the most likely horizon in ambiguous situations, alternative horizons are made by generating the next most likely branch choices from ambiguous points along the horizon, as defined by the spread in heat values among neighboring pixels.

By experiment, overall system performance is increased for parameters $\alpha = 0.5$ (in Equation 3.35) and allowing branches only when $certainty_{pixel} < 0.2$ (in Equation 3.33). The results are in Table 4.16. The error is improved, but only marginally, the reason being the data is generally sufficient for the route. The horizon weighing mechanism is useful for cases where the horizon may go cold, which primarily happens due to missing data. On the other hand, since this approach requires generating five horizons for each point, as well as needing to sum the heat for all pixels within each horizon, the computational load is heightened.

settings	average error	# pixels/nodes
slope in pixel (not decoupled)	9.7% (0.124)	36,600
$lim_{diff} = 0.1$, $lim_{dist} = 50m, min_{dist} = 5m$	11% (0.138)	43,600
$lim_{diff} = 0.1$, $lim_{dist} = 50m, min_{dist} = 10m$	10% (0.129)	32,500
$lim_{diff} = 0.1$, $lim_{dist} = 50m, min_{dist} = 25m$	10% (0.132)	15,900
$lim_{diff} = 0.2$, $lim_{dist} = 50m, min_{dist} = 10m$	11% (0.138)	33,200
$lim_{diff} = 0.0$, $lim_{dist} = 50m, min_{dist} = 10m$	10% (0.134)	58,900
$lim_{diff} = 0.0$, $lim_{dist} = 50m, min_{dist} = 15m$	10% (0.129)	29,500
$lim_{diff} = 0.0$, $lim_{dist} = 50m, min_{dist} = 25m$	10% (0.131)	16,500
$lim_{diff} = 0.05$, $lim_{dist} = 50m, min_{dist} = 25m$	10% (0.130)	16,200
$lim_{diff} = 0.05$, $lim_{dist} = 50m, min_{dist} = 5m$	11% (0.135)	50,800

Table 4.17: The effects of using a decoupled trace merging approach for road grade data

Decoupled road grade map

The use of a decoupled road grade data format is examined. The road grade is saved in a separate quadtree with nodes containing only road slope values and coordinates. These are managed using the trace merging algorithm as described in Section 2.3.1. The parameters are lim_{diff} which is an upper limit for when merging two nodes is considered, and lim_{dist} which is an upper limit for the maximum distance between two nodes to consider merging them. When both these conditions are fulfilled, the nodes are merged. The merging step consists of weighing the slope value with the previous value, as well as computing the average between the node position and the current position.

To avoid noise, when the distance between two nodes is smaller than min_{dist}, they are merged unconditionally. Table 4.17 shows the results of the decoupled road grade approach, for some combinations of parameters.

To conclude, no parameter configuration was found to increase performance by using a decoupled road grade map. The reason might be that input data is too noisy, making the system keep points as separate points whereas the coupled approach will instead minimize the error by unconditionally forming the average value of each data point in the same pixel. It is therefore very hard to find a trade-off that allows flexibility in the decoupled road grade storage while being robust to noisy data.

Some storage can be saved by using a decoupled road grade format, but it does come at a slight cost of accuracy. Since storage is generally not an issue, there does not seem to be compelling reason to use such a format.

Storage

This section contains calculations that determine the storage needed to store a map for use in an HDV. In order to do this, the following assumption is made:

Assumption: A heavy duty vehicle travels 50,000 km of unique road during its lifetime (P. Sahlholm, Ph.D, personal communication).
Equatorial circumference of the earth: 40,075 km.

All figures are quoted in IEC[1] standard format (KiB, MiB, GiB), in which storage prefixes are defined unambiguously as steps of 1024, as opposed to SI standards (KB, MB, GB) which may refer to either steps of 1024 or 1000.

Tile based approach

The tile-based storage used in Pivén and Ekstrand [16] uses 10 bytes per pixel and then stores them in a two dimensional array (tile) within an overarching two dimensional array (the map). Each tile then contains a two dimensional array that contains nxn pixels. The size chosen for this parameter is $200x200$, giving an adequate maximum horizon size within a given set of 9 tiles in memory (see Section 2.3.1). This means each tile will reference 40,000 pixels. In a 32 bit system this means keeping track of 40,000 32 bit (4 byte) memory pointers, for a total of 157 KiB of storage overhead for each tile.

The worst case scenario regarding the amount of tiles necessary is that they are never traveled through diagonally. This gives a minimum coverage of each tile a piece of road of 4 km (using a pixel size of 20x20 meters). Assuming a lifetime travel of a HDV of 50,000 km, the number of tiles needed to store this data is 12,500. This gives a total storage requirement of $12,500 \cdot 157\,KiB \approx 1917\,MiB$. The number of pixels within these tiles would then be $\frac{50{,}000{,}000}{20} = 2,500,000$, giving us a storage requirement of $2,500,000 \cdot 10\,bytes + 1917\,MiB \approx 1940\,MiB$ for the pixels and tiles. The overarching map needs to store a two dimensional array addressing each possible tile, giving us an additional required $\frac{40{,}075\,km}{4\,km} \cdot 4\,bytes \approx 39\,KiB$, which is a negligible amount.

This is a manageable amount, and could furthermore be reduced by purging old data or exceptionally sparse tiles. However, the bulk of storage used consists of pointers that are never used. It is therefore advised to use a smaller tile size if this storage method is to be utilized.

Keep in mind that the calculated figure is a worst-case figure than assumes each tile is only traveled through along a single row or column of pixels. It is likely that each tile would be traveled through in at least two different rows or columns (such as opposing highway lanes), which would bring the data structure overhead to below 1 GiB. In either case, taking this approach will entail storing a large number of sparse matrices.

It is feasible that this amount could be compressed by some suitable compression algorithm thanks to its sparse nature. This can be utilized when swapping to disk, but adds a bit of computational overhead instead.

Using a quadtree

A more flexible and easy to use solution, however, is obtained through the use of a quadtree. It is especially suited to storing sparse data without adding massive memory or computational overhead.

The border length in a quadtree node is halved for each subsequent level. This means that the border length at level i is $\frac{1}{2^{i-1}}$, starting from level 1. Using a maximum number of levels of 20, the bounding box side length of the bottom nodes is $40,075,000\,m \cdot \frac{1}{2^{n_{levels-1}}} =$

$\frac{40{,}075{,}000\,m}{2^{19}} \approx 76\,m$. This bounding box will fit a maximum of 4 pixels along each side (worst case), for a total of 16 pixels per bottom node. This means in the worst case scenario, after finding the appropriate node, 15 pixels need to be searched and discarded before finding the correct one.

Using this data structure also means that additional memory needs to be included in each pixel for storing their coordinate, as this is not unambiguously determined by their location within the data structure. Since $2^{16} < \frac{40{,}075{,}000\,m}{20\,m} < 2^{32}$, 32 bit unsigned integers may be used for this.

Using the data structure as defined in Section 3.9, the final pixel size is 16 bytes. This gives a pixel storage requirement of $2,500,000 \cdot 16\,bytes \approx 38\,MiB$ for the same size pixels.

The worst case scenario would be straight travel through the spatial area. With the previous assumption of 50,000 km of traveled road, this means 3 of the top level nodes would be traversed. The number of bottom nodes is $n_{bottom} = \left\lceil \frac{50{,}000{,}000\,m}{76\,m} \right\rceil = 657,895$. The level above that is half that amount, and the one above that half again, etc. Giving us a total number of nodes:

$$n_{total} = \sum_{i=0}^{N_{levels}-1} n_{bottom}\,\frac{1}{2^i} = n_{bottom}\frac{1-(\frac{1}{2})^{N_{levels}}}{1-\frac{1}{2}} \tag{4.2}$$

Inserting our values gives the result $\sim 1,320,000$. Each node consists of four 32 bit pointers, plus 3 pixel pointers per bottom node, bringing the data structure overhead to $1,320,000 \cdot 16\,bytes + 658,000 \cdot (3 \cdot 4)\,bytes \approx 30\,MiB$. All in all, this map will use approximately $73\,MiB$ of storage.

Chapter 5
Discussion

This chapter contains discussion regarding the most suitable system for route prediction and self-learning map storage. It also presents the reader with a brief overview of the results obtained in this thesis. This chapter can be read independently of the rest of the thesis, provided an understanding of the heat map based system explained in Section 3.4.

System parameters

This section contains discussion regarding the conclusions that were drawn from the system implemented. Since various approaches were implemented, these are compared to each other.

Route prediction approach

A problem with the previous solution, the directional algorithm by Pivén and Ekstrand [16], is that a conflict in road data at the point where the highway passes over another road arises. The same pixel is sometimes passed through on the highway, and sometimes below, each time updating the map with conflicting data. This ultimately leads to the wrong prediction of "jumping off" the highway, as seen in Figure 4.11. An inherent problem with the directional route prediction approach is that the predicted new direction is an average of historical recordings. This means that the predicted direction may be an angle that falls in between two different valid paths, but is itself not a valid path to take, which is what happens in the example. The heat map approach handles complex situations such as this one more gracefully, as shown in Figure 4.12.

Pixel size

A pixel size of 20x20 meters is shown to be the ideal size for the heat map based algorithm (see Section 4.2.1). Because slope data and prediction data are saved in the same pixels, varying the size has several effects. A lower pixel size gives more fine-grained road slope assuming sensors are sensitive enough, and that the predicted route is exact enough to pass through the correct pixel. A smaller pixel size also affects route prediction by spreading the same amount of data over more pixels, resulting in more sparse information to use for route prediction. Another problem that increases as pixels shrink is that the number of possible routes increase. This increases the risk of choosing the wrong path, choosing a dead end path or ending up in some uncommonly traveled through pixel that yields an incorrect prediction.

A larger pixel size, on the other hand, removes errors in route prediction by eliminating the tendency for slightly different routes. Overall, no beneficial effects were found from decoupling the road slope data and route prediction data, and it seems like the concluded size is a reasonable choice for both.

Number of heat maps

For straight highway travel, when there are no road choices, a single heat map works very well. This is because of the limited number of recordings done for each pixel, the fewer directions, the more overdetermined the system will be, leading to more accurate data. When increasing the number of heat maps, the same amount of data is spread out over several layers of heat maps. On the other hand, using a single road map does not allow for intelligent road choice behavior, and for data sets containing road choices the performance will be unsatisfactory.

The best system performance for all references is found for 3 directional heat maps (see Section 4.2.4), assuming the number of previous runs is at least 10. In cases of lower previous runs, the single heat map case may be better for simpler road situations. This is because a higher number of heat maps means spreading out the data more, resulting is more sparse data. Overall, 3 directional heat maps performs well for any amount of previous traces. The largest discrepancy is found for 5 previous traces, resulting in an 8% higher error for 3 heat maps as compared to a single one, for Reference #2, consisting mainly of road segments without crossings. For the other references, however, a single heat map configuration performs significantly worse in all circumstances.

Road grade format

A planar format for storing the road grade as a plane in each pixel is explored (as explained in Section 3.3.3), however turns out to produce a lower performance that the discrete approach of simply storing a value for each directional heat map. One problem with the planar approach is that opposing lanes that are close to each other, such as on rural roads, might have inconsistent road grade but still fall within the same pixel, since a 20 meter pixel width is enough to fit both lanes in the same pixel. This gives rise to inaccurate road grade data and a conflict depending on which direction is traveled most often.

The discrete format, on the other hand, allows the storage of inconsistent data. A pixel should ideally approximate a small enough portion of the road such that the road slope can be considered a plane. However, the reality is such that road slope within a pixel of size 20 meter might very well be inconsistent depending on the direction traveled. Therefore, the discrete approach outperforms that planar format.

Another advantage of the discrete road format lies in its computational lightness; it simply requires recalling one of *n* values (typically 3), whereas the planar approach, while more theoretically elegant, requires numerical computations to find the plane and to recall the road grade in any one direction.

As for the decoupled (node based) road grade format, no parameter configuration was found to increase performance (see Table 4.17). The reason is that the input data is too noisy, making the system keep points as separate points whereas the coupled approach will instead minimize the error by unconditionally forming the average value of each data point in the same pixel. It is therefore very hard to find a trade-off that allows flexibility in the decoupled road grade storage while being robust to noisy data.

Some storage can be saved by using a decoupled road grade format, but it does come at a slight cost of accuracy. Since storage is generally not an issue, there does not seem to be compelling reason to use such a format.

Loops

A loop is defined as passing through the same pixel more than once, giving rise to a “loop” in the predicting route.

Disallowing loops is beneficial to eliminate the risk of looping around on the highway, which is rare, but can happen. However, this means that situations where loops actually occur will now produce an erroneous route prediction. To find a balance between these two design goals, a compromise is made by allowing loops below a certain speed (40 kph is found to be suitable). Experimentation further proves that by allowing a single loop also at higher speeds, in some complex situations the route prediction actually becomes more accurate by being able to loop around and find the correct road in case it temporarily goes in the wrong direction. But limiting loops to one eliminates endless loops. For slow driving (below 40 kph), such as quarries, a higher number of loops yields a better result.

Aging

The aging strategy proves crucial to system performance. It is of the highest importance that the system consistently performs well on commonly traveled road networks. Yet still, an aging strategy is needed in order to keep values from overflowing their data types. The highest performance is achieved by demoting all neighboring heat values with 1 when a heat value reaches a maximum capacity of 32 (results in Section 4.2.7). This means that three heat values (for a 3 direction heat map) can be stored as a single 16-bit integer (explained in Section 3.9).

Distance calculation

For calculating the length in the generated horizon, linear, polynomial and spline interpolation are evaluated (see explanations and figures in Section 3.5). Spline interpolation is done by discarding some points in order not to fit exactly through every point. The problem with this, however, is that curves are cut too tightly, and the distance is generally underestimated. Linear and polynomial interpolation are used by fitting the function to points with some distance between them, calculating arc length and dividing by the number of data points between the selected evaluation points, and then moving this “sliding value” for each new data point. Choosing a distance of five data points proves to give the most accurate estimate.

Quadratic and cubic polynomial interpolation gives a very high error, in comparison, but this is mainly due to their endpoints not passing through actual start and end pixels. Compensating for this using linear interpolation between the end pixels and the polynomial endpoints make them a very close match to the linear approach. Ultimately, however, the linear approach is slightly better and very quick, computationally.

To use spline fitting, some pixels have to be discarded, since the estimated route should not pass the mid point of every single pixel in the horizon. Doing so yields a curve that looks like a reasonable approximation of a plausible route. However, depending on the curvature, it tends to underestimate the travel distance because it cuts corners too early (because pixels are discarded regularly). A possible improvement to this may be a more intelligent pixel dismissal algorithm that finds the pixels farthest into each corner. See complete results in Section 4.2.2.

Horizon transmission

The rate at which the system is updated is coupled to the rate at which new horizons are generated internally. Since these are to be used in another ECU and another software system, they need to be transmitted across the CAN bus. Managing the transmission approach by only sending select messages brings two advantages:

1. Lower bandwidth usage
2. More stable behavior

That sending less data is equivalent to lowered bandwidth usage is obvious, but the second point is more novel. If we re-send the horizon every time, this means the horizon needs to be deleted from the ECU it is used at, and received anew. Because the low bandwidth of the CAN network, this causes a delay because only two data points can be sent per CAN packet. By only re-sending some of the points, or simply adding to the end of the horizon, these moments of missing data can be greatly reduced.

To accomplish this, the new horizon and the previous horizon are aligned so that they data points overlap. This means the new horizon might have one or more new data points at the tail. These will need to be sent. The previous horizon might contain points at its head that have been spatially passed by the vehicle. These will be removed.

The remaining points are examined. If all road slope values that are not identical between the two horizons are replaced in favor of the newer value, performance is not degraded from the naïve approach, and transmission intensity is lowered by 90.5%, to a level of 0.44 kbps. In fact, performance is slightly higher. The reason for this is that the linear approximation method as described in Section 3.5 works more reliably when working on multiple data points, which makes the first few points of each horizon slightly less accurate than the rest. But when moving forward in an existing horizon, the distance calculation is unchanged and thus based on more data points than currently in the horizon.

This rate is easily maintained. As made evident by Figure 4.13 and 4.14, singular horizons with a high number of retransmitted points are exceedingly uncommon, even for challenging quarry conditions, making bottlenecks a non-issue.

Using this strategy for horizon transmission requires a modification to the ADAS Interface Specification, or the manufacturer specific implementation, as resending individual points is currently not supported by the standard. If one is to adhere strictly to the standard, the entire horizon would need to be resent, which in normal highway driving does not affect results too much (see Table 4.13 and Figure 4.13). However, for the quarry driving reference, which represents a more difficult data set, bandwidth is increased from 0.80 kbps to 1.25 kbps, which is still well below the naïve version that transmits 4.69 kbps (see Table 4.14).

The results confirm the natural assumption that subsequent horizons where the route prediction was unchanged are simply moved forward by a new data point at the end. In these cases the other data points will be identical, which is why so much data can be saved by not re-transmitting these data points.

By limiting the maximum number of points to resend, performance in challenging conditions is improved by reducing the risk of a route prediction that changes frequently in uncertain situations. This reduces bandwidth usage dramatically, and allows for the precise control of the maximum allowed number of CAN messages to send for each generated horizon (results in Table 4.15). In the quarry data set, bandwidth usage was somewhat surprisingly reduced by more than half without degrading prediction performance. The reason for this is that the prediction sometimes behaves erratically for a single data points. By disallowing the complete dismissal of the previous horizon at this point, when the prediction finds its way back to the original route, the amount transmitted is greatly limited compared to if a complete retransmission had been carried out.

Computational considerations

In this section are presented the computational requirements and an evaluation of suitability for using the system on the specified target platform.

Lookup

Lookup is performed both when recording data in a pixel and when doing predictions, once for each pixel in the horizon. This is performed using a quadtree data structure.

For each level, a number of comparisons need to be performed to determine which quadrant the pixel falls within (three in the worst case), for a maximum of 60 comparative branches in a 20 level quadtree. At the bottom level, a linear $O(n)$ brute-force search among the pixels is performed. The maximum possible amount of pixels in a single bottom node is very low, however (see calculations in Section 4.7), and this process can be considered constant $O(1)$.

Recording

The recording step always works on the previously passed pixel in order to calculate a current direction as well as a previous direction. This requires one pixel lookup at the previously passed coordinates, and direction calculation between the previous pixel and current pixel giving the current direction. The direction between the previous pixel and the one before that is calculated to determine entrance direction into the previous pixel. In addition to this, linear interpolation between points is used if the vehicle has traveled farther than into a neighbor of the previous pixel.

Each direction is calculated using an arctangent function call, two addition operations and three multiplication operations.

Bresenham's algorithm is then invoked, as explained in Algorithm 3.2. The previous pixel, as well as any "skipped" pixels are then looked up and recorded using the current direction and slope. Using the discrete slope approach, for each pixel, two multiplications are performed to weigh the slope and direction against previously kept values.

The planar approach, on the other hand, involves taking two cross products to find the new normal vector of the plane, as described previously. This uses 6 floating point operations per cross product. This is more computationally intensive, but should be of little concern on the target platform, especially when performed only once a second. It is feasible to implement this using fixed point arithmetic, in order to eliminate floating point operations, but this appear unnecessary.

Horizon generation

The horizon generation begins by finding the succeeding pixel to the one where the vehicle is currently situated. This is done by looking at the neighboring pixels (including diagonal neighbors) and calculating the appropriate heat value for these according to the formula described previously.. Using the current direction, the appropriate heat map is selected and a function call to each of the 8 neighbors performs the heat calculation. Finding the heat for a single pixel uses four multiplication operations and several addition operations to weigh adjacent heat values in order to produce a more stable prediction. To calculate all heat values then requires 24 multiplication operations. They are then compared to each other to find the greatest one. This process is repeated once for each pixel that is added to the horizon, which for a 20 meter pixel size and desired horizon length of 2,500 meters is at most 125 pixels.

The horizon is the aligned with the previous horizon by looking at travel distance estimation of the first few points and finding the most closely overlapping points in the old and new horizons. Any previous values of the old horizons are then discarded. The rest of the elements are iterated through and compared and all points that have changed from the previous horizon are marked for re-transmission and resent, along with one or several new data points that are appended at the end of the horizon. The number of such points depends on the vehicle speed and sample frequency of the horizon generation.

Chapter 6
Conclusions

This chapter presents the viewer with a brief summary of the system developed in this thesis, its performance and the conclusions drawn from this system. The last section in this chapter concerns possible further work within this field.

Summary

After evaluation, the system that yields the highest performance is the novel heat map based map format with three directions of the type described in in detail in Section 3.4. This system predicts the most likely route by storing the frequency at which travel has historically occurred through a raster map in separate heat maps, depending on the current direction of travel. This yields a map system consisting of multiple heat maps, visualized in Figure 6.1, each heat map representing the likelihood of travel, on a pixel level, for a particular heading span.

When driving, the heading determines which one of the three directional heat maps to select, and the heat for the current pixel is increased in this selected direction. When predicting, the heading and heat is used to find the most likely pixel to travel to according to the relevant heat map, and this is iterated for the desired horizon length.

Along with the heat maps, the recorded road slope is also stored for each pixel, on a per direction basis. When the route prediction has been made, the corresponding road slope, for those pixels, is recalled and this represents the final output of the system.

A pixel size of 20x20 meters yields a highly accurate prediction model, as well as modest storage requirements and low computational overhead. This system has been shown to accomplish higher prediction performance than the previous direction based approach for every scenario.

Table 6.1 shows an overview of the system performance using the parameter settings that were found to produce the smallest error. Sample rate is a fixed 1 Hz for both prediction and recording. The percentages cited are defined as fractions of the error when no

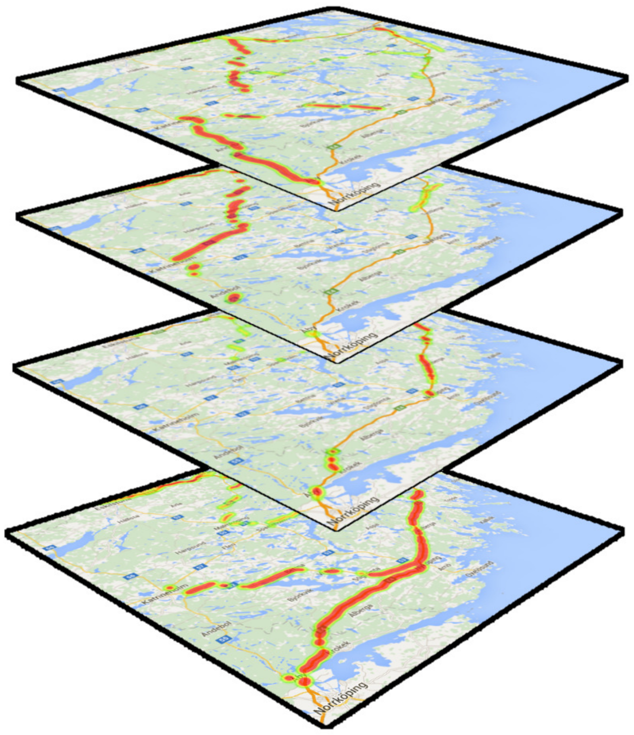

Figure 6.1: A four component directional heat map. Map data: Google. Top to bottom: heading south, west, north and east

Average error, crossings (Reference #1)	26% $\left(\frac{0.430}{1.63}\right)$
Average error, highway and rural (Reference #2)	9.7% $\left(\frac{0.124}{1.28}\right)$
Average error, quarry (Reference #3)	48% $\left(\frac{2.11}{4.43}\right)$
Total road length Reference #2	732 km
Map size Reference #2 (pixels)	36,600
Map size Reference #2 (KiB)	787 KiB
Average bandwidth Reference #2	0.44 kbps

Table 6.1: Performance overview of preferred system

prediction is used. For complete details on the data and other parameters, see Section 4.2. The values were calculated by simulating driving along reference routes and using data collected by HDVs when driving along those routes. See Section 4.1.3 for details on the reference routes.

The recommended data transmission approach is to, rather than send a new horizon at each sample, align the new and old horizons so that their data points overlap as closely as possible. Provided that the route prediction has not changed, this means the new horizon will simple be further ahead spatially. Then, only the points whose slope value has changed are transmitted, including any new points at the tail end of the horizon. This results in a very low bandwidth requirement.

To transform the string of road slope values into a string of road slope values and spatial distance pairs, a travel length estimation is carried out. This is done as a linear interpolation in a sliding window of length five, between the coordinates of the predicted pixels, as this proves to yield the most accurate estimate.

That the error figure for the quarry reference is so high can be explained by the high derivative (noise) of the road grade signal when driving in the quarry, even though the system predicts the route well, as shown in Figure 4.9.

The most common case of HDV operation, rural and highway driving, yields a prediction error of less than 10% in absolute road grade. To achieve this figure, ten previous runs along the route were recorded as input to the system. This represents the performance of the system for a road portion that has been traveled ten times previously.

Storage

Table 6.2 shows a summary of estimated storage figures for using a predictive map throughout the service life of a HDV as calculated in Section 4.7.

The figures of using a quadtree to store the pixels show that storing such a map in the target platform specified in the Background chapter is realistic, and has room to grow. Provided that the commercial map data currently residing in the system were to be removed, there would be room to fit the expected lifetime map of a HDV more than 60 times over, or 3,000,000 km worth of unique road.

This can be compared to the typical life expectancy of a HDV of at least 800,000 km, after which it is often sold and exported for continued use ([7]). All parts of the vehicle are specified with a life expectancy of at least 2,000,000 km. Note, again, that the vehicle is

metric	20x20m tile-based	20x20m quadtree
pixel data	23 MiB	38 MiB
overhead	1917 MiB	30 MiB
total	1940 MiB	68 MiB

Table 6.2: Worst case storage use (uncompressed)

extremely unlikely never to pass the same road twice, in which case storage does not grow. A life expectancy of at the very least 3,000,000 km for this system is more than satisfactory. It is unrealistic to believe that storage may ever run out when using this system with 4 GiB of storage as specified by the target hardware.

Further study

All data used for simulation in this thesis is sampled from higher frequency data by selecting single data points. A more fine-grained simulation of letting the system average higher frequency data may be explored, in the pursuit of reducing sparseness.

The next logical step in the development of a self-learning road slope prediction system for the purpose to look-ahead control would be to implement and test the system shown to produce the highest performance. This would involve rewriting the system in C, taking care to write efficient code, and to implement a CAN communication interface for horizon transmission.

The current production system of using preprogrammed commercial topography maps performs very well compared to the solutions of competitors, which is why an exhaustive performance evaluation compared to the current system is necessary, if a self-learning design is to replace the current system. Another possibility is to investigate the implementation of a hybrid system that combines both approaches.

This thesis looks at using a node based road slope storage approach, but does not use such an approach for storing prediction data as this is incompatible with the algorithm developed for this purpose. Further investigation into using a complete node-based system for prediction is another possible route for further investigation.

Bibliography

[1] Iec 80000-13:2008 quantities and units – part 13: Information science and technology.

[2] J. Biagioni and J. Eriksson. Inferring road maps from gps traces: Survey and comparative evaluation. *91st Annual Meeting of the Transportation Research Board*, 2012.

[3] J. E. Bresenham. Algorithm for computer control of a digital plotter. *IBM Systems Journal 4*, 1965.

[4] S. Durekovic, A. Bracht, B. Raichle, M. Rauch, J. Requejo, D. Toropov, A. Varchmin, D. Balzer, M. Griesbeck, J. Löwenau, S. Marwitz, M. Mittaz, C. Ress, N. Smith, S. T'Siobbel, and M. Wagner. Advanced driver assistance systems interface specifications v2 protocol. ADASIS Forum, April 2010.

[5] S. Fabian. Se1650027-4s (self-learning map), 2016.

[6] R. A. Finkel and J. L. Bentley. Quad trees a data structure for retrieval on composite keys. *Acta Informatica vol 4 issue 1*, 1974.

[7] T. Hällqvist. Scania performance specification - long haulage.

[8] E. Hellström, M. Ivarsson, L. Nielsen, and J. Åslund. Look-ahead control for heavy trucks to minimize trip time and fuel consumption. *5th IFAC Symposium on Advances in Automotive Control*, 2007.

[9] E. Hellström, J. Åslund, and L. Nielsen. Horizon length and fuel equivalents for fuel-optimal look-ahead control. *6th IFAC Symposium on Advances in Automotive Control*, 2010.

[10] F. Hillnertz. Incremental self learning road map. Master's thesis, KTH, 2014.

[11] C. Kinney. Us75263259. 1991.

[12] A-M. Legendre. *Nouvelles méthodes pour la détermination des orbites des comètes*. F. Didot, 1805.

[13] X. Liu, J. Biagioni, J. Eriksson, Y. Wang, G. Forman, and Y. Zhu. Mining large-scale, sparse gps traces for map inference: Comparison of approaches. Technical report, HP Labs, 2012.

[14] J. B. MacQueen. Some methods for classification and analysis of multivariate observations. In *Proceedings of 5th Berkeley Symposium on Mathematical Statistics and Probability*, 1967.

[15] E. Parzen. On estimation of a probability density function and mode. *The Annals of Mathematical Statistics*, 1962.

[16] P. Pivén and O. Ekstrand. Grid based predictive roadmap. Master's thesis, KTH, 2015.

[17] M. Rosenblatt. Remarks on some nonparametric estimates of a density function. *The Annals of Mathematical Statistics*, 1956.

[18] P. Sahlholm. *Distributed road grade estimation for heavy duty vehicles*. PhD thesis, KTH, 2011.

[19] Scania. *Scania Active Prediction - presentation*, 2011.

[20] I. S. Schoenberg. Contributions to the problem of approximation of equidistant data by analytic functions. *Quarterly Applied Mathematics 4*, 1946.

[21] T. Simpson. *Doctrine and Application of Fluxions. Containing (besides what is common on the subject) a Number of New Improvements on the Theory. And the Solution of a Variety of New, and very Interesting, Problems in different Branches of the Mathematicks*. J. Nourse, 1750.

[22] H. Steinhaus. Sur la division des corps matériels en parties. *Bulletin L'Académie Polonaise des Science, Série des Sciences Mathématiques, Astronomiques et Physiques*, 1957.

INSTITUTIONEN FÖR DATAVETENSKAP | LUNDS TEKNISKA HÖGSKOLA | PRESENTATIONSDAG 2016-03-18

EXAMENSARBETE Robust Route Prediction in Raster Maps
STUDENT Sebastian Fabian
HANDLEDARE Flavius Gruian (LTH), Per Sahlholm (Scania CV AB)
EXAMINATOR Jonas Skeppstedt

Saving fuel using a self-learning map

POPULÄRVETENSKAPLIG SAMMANFATTNING **Sebastian Fabian**

To save fuel in trucks, the use of a self-learning map is explored. By predicting the path, and then the road grade for this path, fuel savings can be achieved via intelligent cruise control and gear shift timing.

As competition in the logistics industry hardens, pressure on heavy-duty truck manufacturers to save fuel, and thus costs, reaches unprecedented levels. Fuel-efficient engines no longer being enough, attention increasingly turns to intelligent software solutions. One idea for such a solution is to predict upcoming hills and crests for intelligent cruise control that saves fuel by driving smoothly and avoiding sudden braking.

A self-learning map that uses statistical data to generate a route prediction, and from this prediction a road grade prediction, proves an efficient means to solve this problem. A unique feature of this system is its ability to build a complete map from scratch that contains information about statistical travel as well as topographical data. Each time the vehicle drives along the same road, the information is updated. After 10 such drives the upcoming road slope can be predicted up to 2,500 meters with an average error of less than 10 percent.

As the vehicle drives through a known area, the road grade for the path ahead is predicted. To do this, the path the vehicle will take must be predicted. Then, the road grade for this path is predicted. The end result is a diagram that shows what road grade the vehicle will encounter. By using this information, and for example letting off the throttle before a crest, unnecessary fuel consumption is avoided.

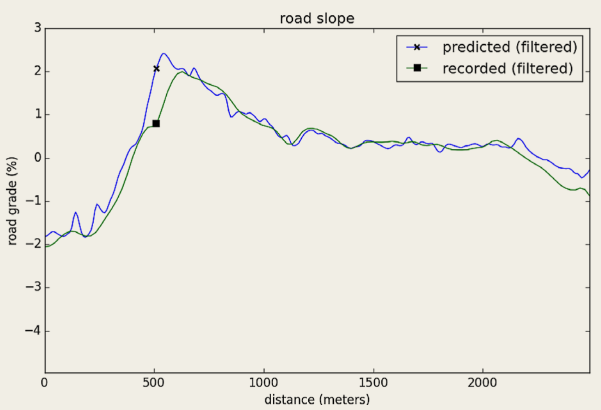

A diagram showing the predicted road grade in percentage points and the actual road grade

At the heart of this system are directional heat maps that store data in frequency grids. The world is divided into small “pixels” of 20 by 20 meters. Each pixel has three layers, divided into three direction ranges. Each pixel contains a value that represents the likelihood of travel through this pixel. The way this works is, when the vehicle drives through a pixel, the pixel corresponding to the current position is selected. Then the direction of travel determines which direction layer to use. Finally, the selected pixel has its value (“heat”) increased by one for this direction.

When doing the prediction, the neighboring pixels are examined to find the one with the highest “heat” for the current driving direction. This pixel is selected as the next prediction, and the process is repeated for the desired prediction length.

The main advantage of this system, as compared to other solutions, is that it does not require any previous knowledge of the road network. This means that it can be used in areas and countries where topographical data is scarcely available. Furthermore, the system is designed in a lightweight manner such that it may be used in embedded automotive hardware already present in all Scania heavy-duty vehicles.